https://doi.org/10.5194/bg-2022-229
Preprint. Discussion started: 20 December 2022

Biogeosciences Discussions

Multi-site evaluation of modelled methane emissions over northern wetlands by the JULES land surface model coupled with the HIMMELI peatland methane emission model

Yao Gao[1,2], Eleanor J. Burke[3], Sarah E. Chadburn[4], Maarit Raivonen[5], Mika Aurela[1], Lawrence B. Flanagan[6], Krzysztof Fortuniak[7], Elyn Humphreys[8], Annalea Lohila[1,5], Tingting Li[9,10], Tiina Markkanen[1], Olli Nevalainen[1], Mats B. Nilsson[11], Włodzimierz Pawlak[7], Aki Tsuruta[1], Huiyi Yang[12], Tuula Aalto[1]

[1]Finnish Meteorological Institute, P.O. Box 503, FI-00101 Helsinki, Finland
[2]Department of Civil Engineering, University of Hongkong, Hongkong, China
[3]Met Office Hadley Centre, Exeter, UK
[4]Department of Mathematics, University of Exeter, Exeter, UK
[5]Institute for Atmospheric and Earth System Research (INAR)/Physics, Faculty of Science, University of Helsinki, P.O. Box 68, 00014 Helsinki, Finland
[6]Department of Biological Sciences, University of Lethbridge, 4401 University Drive, Lethbridge, Alberta, Canada
[7]Department of Meteorology and Climatology, Faculty of Geographical Sciences, University of Lodz, Lodz, Poland
[8]Department of Geography and Environmental Studies, Carleton University, Ottawa, Canada
[9]State Key Laboratory of Atmospheric Boundary Layer Physics and Atmospheric Chemistry, Institute of Atmospheric Physics, Chinese Academy of Sciences, Beijing 100029, China
[10]Southern Marine Science and Engineering Guangdong Laboratory (Zhuhai), Zhuhai 519000, China
[11]Department of Forest Ecology and Management, Swedish University of Agricultural Sciences, 901 83 Umeå, Sweden
[12]Livelihoods and Institutions Department, Natural Resources Institute, Faculty of Engineering & Science, University of Greenwich, UK

Correspondence to: Yao Gao (yao.gao@fmi.fi)

Abstract. Northern peatland stores a large amount of organic soil carbon and is considered to be one of the most significant CH_4 sources among wetlands. The default wetland CH_4 emission scheme in JULES (land surface model of the UK Earth System model) only takes into account the CH_4 emissions from inundated areas in a simple way. However, it is known that the processes for peatland CH_4 emission are complex. In this work, we coupled the process-based peatland CH4 emission model HIMMELI (HelsinkI Model of MEthane buiLd-up and emIssion for peatlands) with JULES (JULES-HIMMELI) by taking the HIMMELI input data from JULES simulations. Firstly, the soil temperature, water table depth (WTD) and soil carbon simulated by JULES, as well as the prescribed maximum leaf area index (LAI) in JULES were evaluated against available datasets at the studied northern wetland sites. Then, the simulated CH_4 emissions from JULES and JULES-HIMMELI simulations were compared against the observed CH_4 emissions at these sites. Moreover, sensitivities of CH_4 emissions to the rate of anoxic soil respiration (anoxic Rs), surface soil temperature and WTD were investigated. Results show that JULES can well represent the magnitude and seasonality of surface (5-10 cm) and relatively deep (34-50 cm) soil temperatures, whereas the simulated WTD and soil carbon density profiles show large deviations from the site observations. The prescribed maximum LAI in JULES was within one standard deviation of the maximum LAIs derived from the Sentinel-2 satellite data for Siikaneva, Kopytkowo and Degerö sites, but lower for the other three sites. The simulated CH_4 emissions by JULES have much smaller inter-annual variability than the observations. However, no specific simulation setup of the coupled model can lead to consistent improvements in the simulated CH_4 emissions for all the sites. When using observed WTD or modified soil decomposition rate, there were only improvements in simulated CH_4 fluxes at certain sites or years. Both simulated and observed CH_4 emissions at sites strongly depend on the rate of anoxic Rs, which is the basis of CH_4 emission estimates in HIMMELI. By excluding the effect from the rate of anoxic Rs on CH_4 emissions, it is found that the Rs-log-normalized CH_4 emissions (log normalization of the ratio of CH4

https://doi.org/10.5194/bg-2022-229
Preprint. Discussion started: 20 December 2022

emission to anoxic Rs rate) show similar increasing trends with increased surface soil temperature from both observations and simulations, but different trends with raised WTD which may due to the uncertainty in simulated O_2 concentration in HIMMELI. In general, we consider the JULES-HIMMELI model is more appropriate in simulating the wetland CH_4 emissions than the default wetland CH_4 emission scheme in JULES. Nevertheless, in order to improve the accuracy of simulated wetland CH_4 emissions with the JULES-HIMMELI model, it is still necessary to better represent the peat soil carbon and hydrologic processes in JULES and the CH_4 production and transportation processes in HIMMELI, such as plant transportation of gases, seasonality of parameters controlling oxidation and production, and adding microbial activities.

1 Introduction

Methane (CH_4) is a powerful greenhouse gas with 33 times the radiative forcing of carbon dioxide (CO_2) over a 100-year time scale (Myhre et al., 2013). Atmospheric emissions and concentrations of CH_4 continues to increase, making CH_4 the second most important human-influenced greenhouse gas (GHG) in terms of climate forcing, after CO_2 (Ciais et al., 2013). Wetland CH_4 emission is not only the single largest but also the most uncertain natural source in the global CH_4 budget (Saunois et al., 2020, Saunois et al., 2016; Denman et al., 2007). As the single largest natural source of CH_4 emission, natural wetlands account for around 20% (149 vs. 727 Tg CH_4 yr^{-1}) to 31% (180 vs. 576 Tg CH_4 yr^{-1}) of global CH_4 emissions estimated from bottom-up and top-down approaches between the year 2008-2017 (Saunois et al., 2020).

The relationship between wetland CH_4 emission and its environmental controls is complex and remains unclear. In general, the controls on wetland CH_4 emission have been demonstrated to be soil temperature, water table depth (WTD) and vegetation. However, these relationships can be modified by wetland types, region and disturbance etc. (Knox et al., 2019; Turetsky et al., 2014). Based on field measured CH_4 emissions, Yvon-Durocher et al. (2014) found a temperature dependence of seasonal variations in wetland CH_4 emissions, which is similar to the temperature dependence of CH_4 production derived from experiments based on pure cultures of methanogens and anaerobic microbial communities. Lupascu et al. (2012) illustrated that a lower water table stimulates lower CH_4 production potentials. However, Zhang et al. (2021) concluded that water level becomes less dominant for CH_4 productions when sampling wetland sites with a wide range of nutrient gradient but similar water level. Recently, Chen et al. (2021) showed that a lower WTD is associated with a decrease in the temperature dependence of CH_4 emissions and a higher WTD has the opposite effect, but WTD does not affect the temperature dependence of CO_2 emissions; i.e., wetland CH_4 emissions may be less sensitive to increasing temperature than CO_2 emissions when WTD is low, which could lead to changes in the ratio of CH_4 to CO_2 emissions and further climate impact (Huang et al., 2021). Moreover, plants provide the major source of organic matter in wetlands and also play an important role as one of the main pathways for methane transport to the atmosphere through their vascular tissues (Dorodnikov et al., 2011).

The strong sensitivity of wetland CH_4 emissions to environmental controls has raised concern on potential positive feedbacks under future climate change (Dlugokency et al., 2009). Numerical models simulating wetland methane emissions with varied complexity have been developed for site- and regional-level and implemented in global climate and carbon cycle models, in order to quantify the magnitude, investigate the spatial and temporal variations, and understand the mechanism and environmental controls of wetland methane emission and its feedback to climate (Xu et al., 2016). Eight global-scale process-based models and two regional models with simple to relatively complex schemes in simulating wetland CH_4 emission were compared in the Wetland CH_4 Inter-comparison of Models Project (WETCHIMP) (Melton et al., 2013). Large divergences (about ±40% of the all-model mean) were found in the modelled annual global wetland CH_4 emissions from the model ensemble

https://doi.org/10.5194/bg-2022-229
Preprint. Discussion started: 20 December 2022

in WETCHIMP. The large variations in simulated CH_4 emission rates were not only due to the uncertainties in wetland areas, but also the parameter and structural uncertainty in large-scale CH_4 emission models. Treat et al. (2018) found that the measured fraction of annual CH_4 emissions during the non-growing season was significantly larger than that predicted by process-based models. Nevertheless, modelling studies show that the potential positive feedback to climate change of wetland methane emissions can reduce the allowed anthropogenic emissions by around 8.0% to maintain the RCP 2.6 temperature threshold (Gedney et al., 2019) and by up to 10% to meet the Paris climate agreement (Comyn-Platt et al., 2018).

Dynamic modelling approaches such as land surface models provide opportunities to investigate the soil-land surface (vegetation)-atmosphere system in an integrated manner. However, the key processes should be appropriately represented in order to improve the accuracy of model simulations. The Joint UK Land Environment Simulator (JULES; Best et al., 2011; Clark et al., 2011) is the land surface scheme of the UK Earth System Model (UKESM) (Sellar et al., 2019), which contributed to the CMIP6 model ensemble used by the most recent IPCC report. In addition, JULES has participated in multi-model comparison projects such as the Inter-Sectoral Model Intercomparison Project (ISIMIP, Rosenzweig et al., 2017) and the Global Carbon Project (Friedlingstein et al., 2019; Saunois et al., 2020). JULES has also been widely used to make global projections on hydrology, permafrost thaw, carbon and methane emissions (Burke et al., 2017b; Chadburn et al., 2015a; Comyn-Platt et al., 2018; Gedney et al., 2019). The original wetland CH_4 emission scheme in JULES is a simple function based on soil temperature and substrate availability, which can be taken from soil carbon, NPP or soil respiration (Gedney et al., 2004). The gridbox mean methane emission from JULES is calculated using the estimated wetland fraction from the TOP-model approach which accounts for saturated surface area within each grid cell (Gedney and Cox, 2003). Recently, a microbial dynamic based wetland methane emission scheme has been included within JULES and it is now capable of reproducing the observed seasonal dynamics of methane emissions in fully saturated wetland sites (Chadburn et al., 2020). However, unsaturated wetlands, not currently included within this model, can also produce CH_4 emissions.

In this work, we coupled HIMMELI (HelsinkI Model of MEthane buiLd-up and emIssion for peatlands) to JULES by using environment variables simulated by JULES to drive HIMMELI. HIMMELI takes into account both microbial (including CH_4 production and oxidation, as well as other aerobic microbe processes) and transport (including diffusion in peat, plant transport, ebullition) processes in a layered one-dimensional peat column, keeping track of the concentration profiles of CH_4, O_2 and CO_2 (Raivonen et al. 2017). A set of model simulations using both JULES and JULES coupled with HIMMELI (JULES-HIMMELI) was performed over six northern wetland sites. The models' performance was evaluated by comparing modelled results and observational data, in order to identify the strengths and weaknesses of JULES-HIMMELI and define a pathway for further model development.

2 Methods

2.1 Site description

Six northern wetland sites located north of 45°N without substantial human influence on ecosystem functioning were selected for this study (Table 1). These sites are spread between the temperate and boreal climate zones. The type of those wetlands includes both fen (five sites) and bog (one site), and their topography varies from relatively flat to hummock-lawn-hollow. Most of the sites are mainly covered by grass, sedge and mosses, but some are also covered by sparse trees, such as the Mer Bleue and Western Peatland sites in Canada. The CH_4 fluxes were measured by eddy covariance (EC) towers at all the sites, with the timeseries length varying from 5 months to 96 months. A short description of each site can be found in Appendix A.

https://doi.org/10.5194/bg-2022-229
Preprint. Discussion started: 20 December 2022

2.2 Measurement data

2.2.1 Meteorological data and other site measurement data

CH_4 fluxes and meteorological data, as well as relevant ancillary data (such as WTD and soil temperature data) were provided by the site principal inverstigators (PIs). In order to prepare the meteorological diving data for the model simulations, the observed meteorological data for the studied sites (including shortwave and longwave radiation, air temperature, relative humidity, precipitation, air pressure, wind speed) were processed to 3-hourly temporal resolution, and then used to bias correct the long-term reanalysis Water and Global Change Forcing Data (WFD) and WATCH-Forcing-Data-ERA-INTERIM (WFDEI) data (Weedon et al., 2010; Weedon et al., 2014) from the gridboxes where the sites are located. The bias correction method is described in Section 2.4 in Chadburn et al. (2017), and the bias corrected meteorological forcing data covers the period from 1901 to 2018. The other in situ data including WTD, soil temperature were averaged to daily values to evaluate the simulation results from JULES. The measured soil carbon profiles at the sites have been collected from literature or databases (Siikaneva fen from Mathijssen et al. (2016), Lompolojänkkä from Mathijssen et al. (2014), Degerö from Osterwalder et al. (2017) and Larsson (2016) and Mer Bleue from Ameriflux datasets (https://ameriflux.lbl.gov/)).

The observed CH_4 fluxes from site PIs are at thirty-minute temporal resolution for Siikaneva, Lompolojänkkä, Degerö Stormyr and Western Peatland 1 sites. For Kopytkowo, the CH_4 flux is given as hourly gap-filled data (Fortuniak et al., 2021). For the Mer Bleue site, the CH_4 flux is at daily time scale (Brown et al., 2014). To derive the daily flux values, the thirty-minute CH_4 flux data were processed as described in Peltola et al. (2019). Firstly, the thirty-minute CH_4 flux data were quality filtered by removing data points with the worst quality flag based on the flagging scheme in Mauder et al. (2013) and with friction velocity below a site-specific threshold if those are available for the site. Then, for the days with data coverage above 29 out of 48 half-hourly data points (minimum 10 data points for sites without a diurnal pattern in CH_4 flux), daily medians were taken to represent the daily flux values. Thus, no explicit gap-filling of individual half-hourly values was done in estimation of daily values. The systematic bias in the derived daily CH_4 fluxes through this method is considered to be insignificant as the magnitude of diurnal patterns in CH_4 fluxes is typically moderate or negligible (Long et al., 2010; Rinne et al., 2018; Peltola et al., 2019). The daily flux values for Kopytkowo are calculated as the daily averages of the gap-filled hourly data.

2.2.2 Sentinel-2 leaf area index (LAI) data

The daily LAI is an input to HIMMELI. In JULES, the daily LAI is updated by multiplying the annual maximum LAI by a scaling factor, which depends on temperature-dependent leaf turnover rates (Clark et al., 2011). The annual maximum LAI can be prescribed in JULES. In this work, we compared the prescribed annual maximum LAI to the annual maximum LAI values derived from the Sentinel-2 satellite data. The daily Sentinel-2 LAI were obtained for 2017-2020 from the Sentinel-2 level-2A (L2A) products using the Google Earth Engine (GEE) and a Python implementation (Nevalainen, 2022) of the LAI algorithm in the Sentinel Application Platform (SNAP) software (Weiss and Baret, 2016). The data influenced by clouds and snow were filtered out according to the scene classification band available in the L2A product. The LAI values for each site were derived for a polygon with homogenized land cover around the site coordinate. The mean and standard deviation of the LAIs in the selected area were calculated to represent the site LAIs. The maximum LAI and its standard deviation of every year was selected from the time series, and then averaged over all the years to obtain the annual maximum LAI and its standard deviation for each site.

https://doi.org/10.5194/bg-2022-229
Preprint. Discussion started: 20 December 2022

2.2.3 Global gridded soil carbon data

Due to the scarcity of the in-situ measured soil carbon density profiles, we also adopted the soil carbon density from the Global Gridded Surface of Selected Soil Characteristics (International Geosphere Biosphere Programme Data and Information System; IGBP-DIS) dataset (Global Soil Data Task Group, 2000). The dataset contains soil carbon density of the top 1 meter of soil at a resolution of 5x5 arc-minutes. The dataset was generated by the SoilData System developed by IGBP-DIS, which uses a statistical bootstrapping approach to link the pedon records in the Global Pedon Database to the FAO/UNESCO digital Soil Map of the World. In this work, the soil carbon densities for the closest coordinates to the sites were compared with the JULES simulated soil carbon density in the top 1 meter of soil. The soil carbon density of the IGBP dataset has been used as the initial conditions for soil carbon at multiple (twenty-four) sites in modeling CH_4 emissions from natural wetlands by a microbial functional group-based CH_4 model (Song et al., 2020).

2.3 Model description

2.3.1 Overview of JULES

JULES is the land surface model of the UK Earth System Model (UKESM) (Sellar et al., 2019). It simulates physical, biophysical and biochemical processes that control the exchange of radiation, momentum, heat, water, carbon and nitrogen fluxes between the land surface and the atmosphere (Best et al., 2011; Clark et al., 2011; Harper et al., 2016; Wiltshire et al., 2021). JULES can be run as a standalone model driven with meteorological forcing data or as the land surface model of UKESM. The JULES version 5.8 release is used in this work.

JULES has a good representation of soil temperature and soil water, especially in cold regions (Chadburn et al., 2015a; 2015b; Chadburn et al., 2017), which are important environmental variables in simulating wetland methane emission. The default wetland methane emission scheme in JULES is a simple function based on soil temperature and substrate (which can be soil carbon, NPP or soil respiration) availability. The simulated methane emission is then multiplied by the wetland fraction of a gridbox to calculate the gridbox mean methane emissions (Gedney et al., 2004). The wetland fraction is calculated as the inundated area within a gridbox by the TOP-model approach (Gedney and Cox, 2003). The default wetland methane scheme (Gedney et al., 2004) has been updated to calculate the total wetland methane emissions from the methane production on multiple vertical soil layers (Comyn-Platt et al., 2018). A more detailed description of the default and updated wetland methane schemes in JULES can be found in Appendix B in Chadburn et al. (2020).

2.3.2 Overview of HIMMELI

HIMMELI (HelsinkI Model of MEthane buiLd-up and emIssion for peatlands) simulates CH_4 build-up in and emission from peat soils (Raivonen et al., 2017). It describes microbial processes (including CH_4 production and oxidation, aerobic respiration) and three transport routes (diffusion in peat, plant transport, ebullition) in a layered one-dimensional peat column, keeping track of the concentration profiles of CH_4, O_2 and CO_2. The model is driven by the rate of anoxic soil respiration (anoxic Rs) for the area of the peatland, soil temperature profile along the soil column, LAI of aerenchymatous peatland vegetation, and WTD. It outputs the CH_4, O_2 and CO_2 fluxes between the soil and the atmosphere, with the ability to separate the contributions of the three different transport routes. Previously, the model has been tested at two Finnish peatland sites (Siikaneva and Lompolojänkkä) and demonstrated its ability to simulate realistic CH_4 fluxes, when run with a combination of measured and simulated site-specific inputs (Raivonen et al., 2017). In this work, the HIMMELI v1.0.1 (i.e. the original version with a few bug corrections) and its default configuration is adopted.

https://doi.org/10.5194/bg-2022-229
Preprint. Discussion started: 20 December 2022

2.3.3 Simulation setup

Seven different model simulations were performed in order to find out the most suitable setup for predicting methane flux at each site (Table 2). In the following text and result figures, the model simulations are referred to with their names in Table 2.

The baseline JULES simulation mainly follows the configuration in Chadburn et al. (2020), which was originally derived from the JULES-ES configuration (see https://jules.jchmr.org/content/core-configurations). The model was set up with a 14-layered soil column of around 3 meters for both hydrothermal and carbon dynamics, as well as the vertically- resolved methane production scheme. The nitrogen scheme was switched off. To improve the representation of the northern wetland sites, the plant functional type (PFT) was prescribed as 100% C3 grass to represent pristine northern wetlands (note there is no PFT to represent moss in JULES yet); the maximum LAI for C3 grass was changed to be 1.3 instead of 3, according to the site measured LAI at summer at Lompolojänkkä (Aurela et al., 2009); and the soil parameters impacting soil hydrology were adjusted (except for Mer Bleue site) to improve the simulated WTD. JULES was spun up to equilibrium of soil hydrothermal and carbon quantities by repeating the forcing data from 1900-1920 for hundreds of times, and then run until the end of 2018.

JULES was also run for all sites with a modified soil carbon decomposition rate (named JULES_$Rs_{modified}$), following an adjustment to the decomposition function of soil moisture content (Section 2.2 in Chadburn et al. (2022)). This modified decomposition function leads to a suppressed decomposition rate (reduced from 60%–85% to 20% of its maximum rate) under saturated conditions, and zero decomposition rate at zero soil moisture content (instead of 20% of its maximum rate). In addition, we tested additional site-specific runs at Siikaneva, Lompolojänkkä and Kopytkowo. At Siikaneva, we prescribed the soil wetness in the JULES soil layers according to the observed WTD at daily time scale, as Siikaneva has the most WTD data available in all the sites (JULES_$Rs_{modified}$_$SW_{prescribed,}$ Table 2). This means the soil layers below the observed WTD were set to be saturated, while the soil moisture above the observed WTD is equal to the simulated one from the baseline JULES runs. By doing this, the simulated soil temperature changes with the observed WTD and the effect of the water table bias on methane emission simulations was removed. It should be noted that fixing the soil wetness to the observed WTD violates the water mass conservation of the model. At Lompolojänkkä, the soil wetness was set to saturated for the entire run, because it is almost saturated throughout the year and only occasionally falls below the surface WTD in summer (JULES_WTD_0). Finally, at Kopytkowo, the LAI_{max} was set to be 2.35 based on the Sentinel-2 LAI data (JULES_LAI_{max}).

In the coupled model of JULES and HIMMELI, the soil and vegetation dynamics of a site (gridbox) simulated by JULES are used to drive HIMMELI. The rate of anoxic Rs of the site, which is not directly simulated by JULES, was calculated as the rate of total soil respiration under the JULES simulated WTD. The simulated soil temperature profile along the prescribed soil layers in JULES was interpolated to match the soil layers in HIMMELI. In the default coupling between JULES and HIMMELI (JULES+HIMMELI), the WTD simulated by JULES was used as an input to HIMMELI. In the HIMMELI_WTD_{obs} simulation, the observed WTD (WTD_{obs}) at site was used as the input to HIMMELI model, and the rate of anoxic Rs of the site was calculated as the total soil respiration rate below the WTD_{obs}. In the JULES_$Rs_{modified}$_$SW_{prescribed}$ + HIMMELI_WTD_{obs} run for Siikaneva, the soil wetness was prescribed according to the observed WTD and the soil temperature simulated by JULES is consistent with the WTD_{obs}.

3 Results and discussion

In this section, we firstly evaluated the JULES simulated soil temperature, WTD and soil carbon density profile, as well as the

https://doi.org/10.5194/bg-2022-229
Preprint. Discussion started: 20 December 2022

prescribed LAI in JULES with site measurements and satellite data. Then, we compared the simulated CH_4 fluxes from different setups of the coupled model to the observed CH_4 fluxes. Moreover, sensitivities of site methane emissions to the rate of anoxic Rs, WTD, and surface soil temperature were studied and compared between observations and modelled results. In this way, we analyzed the potential for improving the coupled model in simulating CH_4 fluxes at northern wetland sites.

3.1 Comparison between simulated and observed environmental variables

3.1.1 Soil temperature

To compare the simulated and observed soil temperatures, the simulated vertical soil temperature profile in JULES was linearly interpolated to the soil temperature observation depth. Taylor diagrams show the evaluation of the simulated soil temperature at the studied sites (Fig. 1). The simulated soil temperature at both shallow (5-10 cm) and relatively deep (34-50 cm) soil depth show strong correlation ($R \geq 0.9$) with the observed soil temperatures at all the sites. All data points are located within the root mean square error (RMSE) circle of 0.6. The ratio of standard deviation demonstrates the difference in the standard deviations between the simulated and observed soil temperatures, where the reference point is 1.0. For most of the studied sites, the ratio of standard deviation is close to the reference point. For the soil temperature at shallow soil depth, the ratio of standard deviation for Kopytkowo (1.24) is the furthest from the reference point due to both the slight overestimation of summertime soil temperature and underestimation of wintertime soil temperature by JULES. This can be attributed to the underestimation of WTD by JULES at Kopytkowo. For the soil temperature at deeper soil depth, the ratio of standard deviation for Degerö is 0.7, which is the smallest one among the sites. Both the shallow and deep soil temperatures at the Degerö site were underestimated throughout the year. The maximum daily difference between model and observations at Degerö reaches 10.25°C in the deep soil temperature in the summer of 2013 of three years data (2013–2015). The observed soil temperature in winter was mainly above zero, while the simulated soil temperature is below zero. The observed WTD in wintertime at the Degerö site is missing (Fig. 2), but it can be speculated that the observed WTD is much higher than the simulated WTD according to the measured WTD in the end of autumn and at the beginning of spring. For sites with saturated soil moisture in wintertime (Siikaneva, Lompolojänkkä and Kopytkowo), the soil temperature is underestimated as the simulated soil was unsaturated. This simulated drying of the soil is because excess water becomes surface runoff from the top soil layer or subsurface runoff from the bottom layer when the soil column is saturated in JULES, instead of ponding. For the MerBleue site, the soil temperature in the winter of 2011 was also underestimated in JULES but the simulated WTD is higher than the observed WTD. This difference in soil temperature can be attributed to the underestimation of the snow depth by JULES in 2011 winter at Mer Bleue (figure not shown). The timeseries of soil temperature at all the sites can be seen in Fig. S1 in supplementary.

3.1.2 Water table depth

The simulated daily WTDs show deviations from the observed WTDs at the studied sites (Fig. 2). Overall, the simulated WTD is lower than the observed WTD at Siikaneva, Lompolojänkkä, Kopytkowo and Degerö sites, but is slightly overestimated at Mer Bleue and Western Peatland 1 site. At Siikaneva, the water table drawdown from the saturated soil in spring to the lowest point in summer is mostly well captured, however, the water table draw up process in the second half of year is much delayed. Lompolojänkkä is a site with almost saturated soil in the period of 2006 to 2011. WTD was below zero only in the summer of 2006. However, as the default JULES hydrology scheme is not able to simulate continuously saturated soil or store extra stagnant water above the surface, and there are no lateral flow inputs to the soil column, the WTD drops when the temperature increases and only becomes saturated in a short period after snow melt in the model. In order to simulate the soil water and WTD at Lompolojänkkä more realistically, we set soil to be always saturated in JULES in JULES_WTD_0+HIMMELI run. Although

https://doi.org/10.5194/bg-2022-229
Preprint. Discussion started: 20 December 2022

the water mass was not conserved in this way, the soil temperature was better simulated under the saturated condition (as shown in Fig. S1). The Kopytkowo and Mer Bleue sites both show strong correlations with the observed WTD (R=0.75 for both sites), but the bias at Kopytkowo site (bias = -0.42 m) is much larger than the bias at Mer Bleue site (bias = 0.06m). The WTD at Kopytkowo site is generally underestimated by JULES, and the very dry years in 2015 and 2018 where the observed WTD is 0.8 m below the surface (mean value of observed WTD is -0.14m from 2013 to 2018) are not captured by the model. The very dry summer in 2012 at Mer Bleue site is not captured by the model either. The simulated WTD at the Degerö site shows negative correlation with the observed WTD, which is mainly because the simulated WTD keeps dropping down in the summer of 2013, whereas the observed WTD raised up slightly. The dynamic of simulated WTD at Western Peatland 1 site is in line with the observed WTD, but the simulated WTD is with slightly higher values (Bias = 0.07m) than the observed WTD.

3.1.3 Leaf area index (LAI)

Compared to the annual maximum LAI values derived from Sentinel-2 satellite data, the prescribed maximum LAI in our simulation is lower for most of the sites except for the Degerö site. The prescribed maximum LAI is close to the Sentinel-2 maximum LAI at the Degerö site and falls in the standard deviation ranges of the Sentinel-2 maximum LAIs at Siikaneva and Lompolojänkkä. However, the Sentinel-2 maximum LAIs at Kopytkowo, Mer Bleue and Western Peatland 1 sites are higher than the prescribed maximum LAI in JULES. The annual maximum LAIs derived from Sentinel-2 satellite data may have some uncertainties due to uncertainties in the used LAI algorithm and atmospheric correction or selection of representative area. Chadburn et al. (2017) showed that simulating correct LAI is important to produce the correct order of magnitude of carbon fluxes, and the vegetation phenology and dynamics could be improved to simulate realistic LAI. The biases in LAI could impact the carbon fluxes simulated by JULES and also the transport capability of CH_4 and O_2 in HIMMELI in this work. As the prescribed and Sentinel-2 maximum LAI at Kopytkowo showed the biggest difference in all the studied sites, a site specific simulation (JULES_LAI_{max}+HIMMELI_WTD_{obs} in Table 2) with Sentinel-2 maximum LAI was set for this site and the impacts on simulated CH_4 flux are shown in Section 3.2.

3.1.4 Soil carbon

The vertical distributions of soil carbon density from the JULES simulations were compared with the available measured soil carbon density profile at four studied sites (Fig. 4). The JULES simulated soil carbon profiles decrease steeply with depth. However, the observed soil carbon density profiles show higher soil carbon densities at the deeper soil depths which is quite different to the simulated soil carbon profiles. Chadburn et al. (2017) also showed that JULES cannot simulate peat soil carbon profiles, and thus a new approach to simulate peat accumulation, degradation and stability has recently been introduced into JULES in Chadburn et al. (2022). In this work, we only adopted the new decomposition function in JULES_$Rs_{modified}$ runs, which does not by itself improve the simulated vertical profile of peat soil carbon and soil respiration. It will be highly interesting to assess how the simulated soil carbon profiles of our study sites will change when using the newly introduced peat soil carbon module in JULES, and how this impacts the methane emissions. This will be addressed in future work.

The averaged soil carbon densities of the top 1m soil carbon from JULES and from IGBP-DIS data, as well as from the observed values at Degerö and Mer Bleue sites are also illustrated in Fig. 4. The soil carbon of the top 1 meter in JULES is overestimated at Degerö site when compared to observation, but agrees with the observations in Mer Bleue site. This differs from Chadburn (2017), where the simulated top 1 meter soil carbon stock was underestimated due to the underestimation of vegetation productivity at most of the studied sites. The comparison of the top 1 meter soil carbon from JULES and IGBP-DIS data for all

https://doi.org/10.5194/bg-2022-229
Preprint. Discussion started: 20 December 2022

the sites are shown in Fig. 5.

3.2 Simulated vs. observed CH4 fluxes

Fig. 6 shows the observed and simulated time series of CH_4 emissions at the sites. The inter-annual variability of the CH_4 flux simulated by JULES is much smaller than that of the observed CH_4 flux in general (Table 3). This is likely caused by the lack of direct WTD dependence of CH_4 emissions in JULES. The variable wetland fraction (Fwet) in a gridbox in the default JULES methane module could dampen the inter-annual variability as only saturated areas are considered to be wetlands in JULES. In addition, Fwet is a gridbox based variable and not designed for site simulations. In reality, the topsoil of wetland is not always saturated and this fluctuation of WTD can impact CH_4 emission in wetlands. The JULES+HIMMELI simulations include this dependence but the simulated CH_4 fluxes are generally smaller than the observed CH_4 fluxes. The main reason is that the simulated WTDs are typically too low (Fig. 2). When using the observed WTD (for Lompolojänkkä, WTD was set to the soil surface, or 0 m) and the corresponding anoxic Rs rate simulated by JULES as the inputs to HIMMELI (JULES+HIMMELI_WTD_{obs}), the simulated CH_4 fluxes increased to values higher than the observations for Siikaneva, Lompolojänkkä, Kopytkowo and Degerö. In addition, the RMSEs between model and observations increased for all sites except for Lompolojänkkä in comparison to the JULES+HIMMELI run. The inter-annual variabilities of the simulated CH_4 fluxes from the JULES+HIMMELI simulations at Siikaneva, Lompolojänkkä and Kopytkowo were smaller compared to the observed CH_4 flux, especially at Kopytkowo site (Table 3). When using the observed WTD in HIMMELI, the inter-annual variabilities at those three sites increased, but too high for Siikaneva and Kopytkowo sites. In this work, we used the default model parameter values for HIMMELI, where the fraction of anaerobic respiration becoming methane (fm) was 0.5. The value of fm affects CH_4 generation and CH_4 emission rate in HIMMELI directly, and the range for fm can vary from 0 to 0.7 (Nilsson and Öquist, 2009). For the underestimated CH_4 emission rates in our JULES+HIMMELI simulations, increasing the value of fm in HIMMELI could decrease the biases in simulated CH_4 emission rates, but would not change the seasonal dynamics of simulated CH_4 emission rates.

When the modified soil decomposition rate was adopted in JULES (as introduced in section 2.3.3.), the overestimated CH_4 flux by JULES+HIMMELI_WTD_{obs} at Lompolojänkkä (Bias changed from 0.13 to -0.53) and Degerö (Bias changed from 0.18 to -0.13) reduced a lot. This reduction was, however, smaller at Siikaneva (Bias changed from 0.52 to 0.42) and Kopytkowo (Bias changed from 0.77 to 0.76) sites. This is partly because the observed WTD, especially the lowest values in summer, at Siikaneva and Kopytkowo are too deep to lead to a notable decrease in the anoxic Rs rate calculated with the observed WTD and the JULES simulated soil respiration profile which decreases exponentially with depth (Fig. 4). In addition, when using the modified function of soil carbon decomposition rate in JULES, the soil respiration in the near surface soil layers can increase when the soil is unsaturated (Fig. S2 in supplementary). Therefore, when using the observed WTD to derive the anoxic Rs rate, the simulated anoxic Rs rate and CH4 flux in Siikaneva and Kopytkowo do not show obvious changes. For Lompolojänkkä, the modified decomposition factor leads to large decreases in CH_4 fluxes due to the decreased soil respiration in saturated soil (Fig. S2 in supplementary). However, this leads to too small CH_4 fluxes compared to the observed CH_4 emissions at Lompolojänkkä, except the summer peak values in year 2010.

The JULES_$Rs_{modified}$_$SW_{prescribed}$+HIMMELI_WTD_{obs} run for Siikaneva simulated much more realistic methane emissions in summertime than the JULES_$Rs_{modified}$ +HIMMELI_WTD_{obs} run. This is due to the changes in soil temperature and anoxic Rs rate when the vertical distribution of soil water is prescribed in JULES. However, the JULES_LAI_{max}+HIMMELI_WTD_{obs} simulation only improves the simulated CH_4 emissions slightly at Kopytkowo. Higher LAI could lead to an increase in litter

https://doi.org/10.5194/bg-2022-229
Preprint. Discussion started: 20 December 2022

input which would mean higher CH_4 substrate. However, here the simulated CH_4 emissions decreased slightly which is due to the increased plant transport of O_2 into the soil with higher LAI (Raivonen et al., 2017). The higher O_2 concentration can increase the CH_4 oxidation and also the O_2 inhibition effect in methanogenesis (Fig. S3 (c,d) in supplementary).

3.3 Sensitivity of (observed and simulated) site methane emissions to the rate of anoxic soil respiration, surface soil temperature and water table depth

The measured CH_4 fluxes of Siikaneva, Kopytkowo and Lompolojänkkä are of relatively long duration and the quality of data is good, therefore those three sites are selected for further investigation of the sensitivity of CH_4 emissions to the rate of anoxic Rs, soil temperature, WTD and LAI.

From Fig. 8, we can see that the simulated CH_4 emissions largely depend on the rate of anoxic Rs. This is consistent with the findings from the sensitivity tests of input data to the standalone HIMMELI, which showed that anoxic Rs rate and the corresponding potential methane production rate (PMP; the methane production rate in conditions with no O_2) determine the output CH_4 emissions and the other factors (LAI and WTD) only modestly modify the methane emission in the model (Raivonen et al., 2017). Thus, it is crucial to have a realistic anoxic Rs rate as the input to HIMMELI. Due to the lack of measured anoxic Rs rate, in Fig. 8, the observed CH_4 emission was plotted against anoxic Rs rate from the simulation showing the strongest correlation with the observed CH_4 emissions in Fig. 6. Therefore, the anoxic Rs rate calculated with JULES simulated WTD was chosen for Siikaneva, and the anoxic Rs rate from the JULES_WTD_0 + HIMMELI was taken for Lompolojänkkä. For Kopytkowo, the anoxic Rs rate from JULES + HIMMELI_WTD_{obs} were adopted. Interestingly, Fig. 8 shows the observed CH_4 emission have linear dependencies on the anoxic Rs rate as well as the simulated CH_4 emission. For Siikaneva and Lompolojänkkä, the linear dependencies between observed and simulated CH_4 emissions are similar. However, for Kopytkowo, the slope between the observed CH_4 emission and anoxic Rs rate is lower than the slopes between the simulated CH_4 emission and anoxic Rs rate due to the overestimation of the simulated CH_4 emission. The linear dependencies of CH_4 emissions on anoxic Rs from both simulations and observations illustrate that it is reasonable to adopt the rate of anoxic Rs as the basis of CH_4 emission estimates in HIMMELI.

Based on the linear dependencies of CH_4 emissions and anoxic Rs rates shown in Fig. 8, we normalized CH_4 emissions by applying the log normalization of the ratio of CH4 emission to anoxic Rs rate (called Rs-log-normalized CH_4 emissions from here on). Fig. 9 shows the dependence of Rs-log-normalized CH_4 emissions on soil temperature for the upper soil layer and WTD from both observation and model simulations at Siikaneva and Kopytkowo sites. We show that the Rs-log-normalized CH_4 emissions increase with increased upper layer soil temperature from either observations or simulations at both sites. This means temperature can impact methane emissions in other way in addition to the rate of anoxic Rs. In HIMMELI, temperature can affect the CH_4 production through inhibition process, the CH_4 oxidation from the dissolved O_2, and the solubility of CH_4 (Raivonen et al., 2017). In cold temperature, the solubility of gases, and thus the concentrations of dissolved O_2 in water is higher than in warm temperature. Therefore, CH_4 oxidation and inhibition of CH_4 production are higher in low temperatures than in warmer temperatures although the rates of these reactions are lower (Fig. S3 in supplementary). The steady state tests (fixed anoxic Rs and WTD inputs) of HIMMELI also showed that a 1°C increase in peat temperature increased the total methane emissions on average by 0.01-0.02% without gas-transporting vegetation and 0.3% with vegetation (Raivonen et al., 2017). Apart from the concentration of both CH_4 and O_2 (Watson et al., 1997), laboratory experiments have shown that CH_4 oxidation is also limited by factors that affect the microbial activity, such as temperature (Whalen and Reeburgh, 1996). Chadburn et al. (2020) developed a wetland CH_4 emission scheme that takes into account methanogenic growth and dormancy (quantity and

https://doi.org/10.5194/bg-2022-229
Preprint. Discussion started: 20 December 2022

activity of methanogens), and concluded that microbial dynamics strongly influence the seasonal cycle of wetland CH_4 emissions. Riley et al. (2011) showed that CH_4 production is more likely to be temperature sensitive than oxidation when methanogens are not substrate-limited, although oxidation rate increases with temperature according to Q10 function.

The Rs-log-normalized CH_4 emissions decrease with rising WTD for Siikaneva from both observation and simulations. The reason can be mainly attributed to three aspects. First, the WTD and surface soil temperature are anti-correlated in general (upper panel in Fig. 10). Second, the root mass available for transporting O_2 into the CH_4 producing peat layer is at its lowest when WTD is the deepest. Third, the diffusivity of CH_4 in water is lower than that in the air (Tang et al., 2010). For the Kopytkowo site, the Rs-log-normalized CH_4 emissions show a slight increase with rising WTD from simulations, when observed WTD was used as the inputs to HIMMELI. In contrast, it shows a slightly decreasing trend with rising WTD in the observation. We have excluded the anoxic Rs effects in the Rs-log-normalized CH_4 in Fig. 9, so we can not attribute the slightly increasing trends to the overestimated CH_4 emissions when WTD is close to the surface and the temperature is high (lower panel in Fig. 10). However, there are two specific drought years (2015 and 2018) in the study period for Kopytkowo, where the lowest WTD happened in October but the temperature had already dropped after the summer (Fig. 3 in Fortuniak et al. 2021). For those two drought events, the low WTD decreases the amount of O_2 transported into the soil but the lower temperature in autumn compared to summer leads to a higher amount of dissolved O_2 in HIMMELI.

When adjusting the maximum LAI to be higher, the simulated CH_4 emissions decreased slightly at Kopytkowo in the HIMMELI simulation (Fig. 6 (c) and Fig. 8 (c)). A greater LAI means a higher CH_4 substrate input in the model and a higher plant transport capacity of CH_4. However, the higher LAI can also increase the O_2 transported into the soil, and thus leading to higher amount of the inhibition of CH_4 production and oxidized CH_4. Here the effect of plant transported O_2 into soil layers is strong with higher LAI, and as a result, the CH_4 emissions decreased slightly as we can see from Fig. 9 (c, d).

4 Conclusions

In this study, a process-based wetland CH_4 emission model HIMMELI was coupled with a current state-of-art land surface model JULES. The evaluation of the coupled model (JULES-HIMMELI) was then performed comprehensively at six northern wetland sites. It is found that the coupled model does not lead to significant improvements in the simulated CH_4 emissions in comparison to the default wetland CH_4 emission scheme in JULES. Nevertheless the coupled model is considered to be more realistic in simulating wetland CH_4 emissions as HIMMELI simulates CH_4 production, oxidation and transportation by vascular plants, ebullition and diffusion in a vertical soil column, while the default wetland methane emission scheme in JULES only takes into account CH_4 emission from saturated wetlands in a simple way.

The CH_4 emissions simulated by the coupled model strongly depend on the rate of anoxic Rs, which represents the CH_4 substrate production rate in HIMMELI. The observed CH_4 emissions are also strongly correlated to anoxic Rs, confirming our model results and underlining the importance of the underlying CH_4 substrate production rate in driving the methane fluxes. It is also found that, after excluding the anoxic Rs effect, O_2 concentration in the peat is an important player in simulating CH_4 emission in terms of the changes in soil temperature, WTD and LAI. Therefore, more realistic representations of peat soil carbon and peat hydrology processes, especially WTD, as well as wetland vegetation (including moss) are needed to improve the simulated wetland CH_4 emissions by JULES-HIMMELI. Recently, a new approach in simulating peat dynamics (accumulation, degradation and stability) has been integrated in the vertically-resolved soil carbon scheme in JULES (Chadburn et al., 2022).

https://doi.org/10.5194/bg-2022-229
Preprint. Discussion started: 20 December 2022

Distributed representation of WTD may also be simulated by the microtopography and ponding scheme developed for JULES (Smith et al., 2022). Implementing those new schemes in the future JULES-HIMMELI model simulations may improve the simulated wetland CH_4 emissions. Furthermore, observed O_2 data in peat soil for validation are largely lacking and expected to be included in future observations.

Appendix A: site descriptions

1) Siikaneva

The Siikaneva site (N, E, m a.s.l.) is a boreal oligotrophic fen site located in Ruovesi in southern Finland (Rinne et al., 2007). The peat depth at the site is from 2 to 4 m. The dominant vegetation of the site includes sedges (C. rostrata, C. limosa, E. vaginatum), Rannochrush (Scheuchzeria palustris) and peat mosses (Sphagnum balticum, S. majus, and S. papillosum). The annual mean temperature of 3.3 °C and precipitation of 713 mm have been measured at the nearest long-term weather station during the period 1971 to 2000 (Drebs et al., 2002). For a more detailed description of Siikaneva, see Aurela et al. (2007) and Rinne et al. (2007).

2) Lompolojänkkä

The Lompolojänkkä site (N, E, m a.s.l.) is an open, pristine and nutrient-rich sedge fen located in northern Finland. The peat depth at the site is up to 3 m at the center of the fen. The vegetation layer at the site is relatively dense and dominated by Betula nana, Menyanthes trifoliata, Salix lapponum and Carex spp. with the mean vegetation height of 40 cm. The mean annual temperature averaged over the period 1971-2000 at the nearest long-term weather station is 1.4 °C (Pirinen et al., 2012). A small stream flows through the site and brings water to the site. The soil at this site is almost continuously saturated throughout the year. More detailed description of Lompolojänkkä can be found in Aurela et al. (2009); Lohila et al. (2010).

3) Degerö Stormyr

The Degerö Stormyr site (N, E, 270 m a.s.l.) is an undisturbed mixed acid mire system situated in the Kulbäcksliden Experimental Forest in Northern Sweden. The mire is situated on high land between two major rivers, the Umeälven and Vindelälven, approximately 70 km from the Gulf of Bothnia. The mire system is composed of interconnected smaller mires divided by islets and ridges of glacial till (Nilsson et al., 2008). The peat depth of the site is mainly between 3 and 4 m, but depths of 8 m have also been measured. The deepest peat depth corresponds to an age of 8000 years. The footprint of the measured CO_2 and methane fluxes is from a minerogenic oligotrophic mire. The vegetation is dominated by lawn (S. balticum Russ. C. Jens and S. lindbergii Schimp.) and carpet (Sphagnum majus Russ. C. Jens) plant communities, as well as vascular (Eriophorum vaginatum L., Trichophorum cespitosum (L.) Hartm., Vaccinium oxycoccos L., Andromeda polifolia L. and Rubus chamaemorus L., with both Carex limosa L. and Schezeria palustris L. occurring more sparsely) plant community.

4) Kopytkowo

The Kopytkowo site (53°35′30.8″ N, 22°53′32.4″ E, 109 m a.s.l.) is a mire located in a large flat area of the Middle Biebrza Basin in northeastern Poland. The depth of peat in this area reaches 2.5 m. The soil of the mire around the site was slightly decomposed due to dehydration. The dominant vegetation around the site is a mixture of reeds, sedges and rushes. The wetlands of Biebrza National Park experienced melioration treatments in the 19th and 20th centuries. In the mid-nineteenth century, the wetlands first drained to intensify agriculture in the region. This human activity has caused partial degradation of the wetland

https://doi.org/10.5194/bg-2022-229
Preprint. Discussion started: 20 December 2022

peat and the natural succession to trees and shrubs was accelerated. In 1993, the Biebrza National Park was established and restoration work has been conducted to restore the original hydrological conditions. The climate of northeastern Poland is temperate with continental influences, with relatively cold winters and warm summers. More detailed descriptions can be found at Fortuniak et al. (2017) and Fortuniak et al. (2021).

5) Western Peatland 1

The Western Peatland 1 site (N, E, m a.s.l. 54.953841N, 112.466981W) is an undisturbed moderately "rich" fen – rich in species richness, not nutrient availability (Flanagan and Syed, 2011). The area around the site is quite flat and with relatively homogeneous vegetation in around 1.5 to 2 km in all directions, except in the north where upland aspen forest shows in around 1 km away from the measurement site. The site is dominated by stunted trees (Picea mariana and Larix laricina), abundant tall shrubs (Betula pumila), and a wide range of moss species, including Sphagnum spp. (S. angustifolium, S. fuscum, and others), brown moss species (Drepanocladus aduncus, Aulocomium palustre, and others) and a feather moss species (Pleurozium schreberi). There are also several herbs and dwarf shrubs with aerenchyma tissue (Triglochin maritima, Menyanthes trifoliata, and Carex spp.) exist in the area. The total leaf area index for the site was 2.6 ± 0.16 m^2/m^2. The total ecosystem carbon stock is 51 kg C/m^2, which is dominated by carbon accumulated in below-ground peat. The above ground live plant tissue is only about 1% of the total ecosystem carbon stock which is contributed by the two tree species. The mean annual temperature and precipitation at the nearest weather station were 2.1 °C and 504 mm averaged over 1971-2000. Detailed descriptions of vegetation and site characteristics were previously provided by Syed et al. (2006) and Long et al. (2010).

6) Mer Bleue

The Mer Bleue site (5.41 N, 75.52 W) is an undisturbed ombrotrophic bog located east of Ottawa, Canada. The peat depth of the site varies from 5 to 6 m at the center and 0.3 m at the edges. The surface of the area of the flux tower is dominated by hummock microtopography (75% of the area) with approximately 25 cm between the tops of hummocks and interhummock spaces (Brown et al., 2014). The vegetation of the site is dominated by evergreen and deciduous shrubs, and Sphagnum mosses (Lafleur et al., 2005). The mean annual temperature is 6.4 ± 0.8 °C, and annual precipitation is 943 mm averaged over 1981-2010. The site has hosted a long-term carbon cycle research program since 1998. For more detailed site description, see Moore et al. (2002), Lafleur et al. (2003) and Roulet et al. (2007).

Data and code availability

The datasets generated and/or analysed during the current study are available from the corresponding author on reasonable request. The in-situ measurement data, including the CH_4 flux and meteorological data as well as other ancillary data can be requested from the site PIs. The tool for deriving Sentinel-2 LAI data is in an open GitHub repository (https://github.com/ollinevalainen/satellitetools, https://doi.org/10.5281/zenodo.5993292, Nevalainen, 2022). The Global Gridded Surfaces of Selected Soil Characteristics (IGBP- DIS) data set is accessible at http://daac.ornl.gov. HIMMELI model source code can be required from Maarit Raivonen (Raivonen et al., 2017). JULES model code and the files for running it are available from the Met Office Science Repository Service: https://code.metoffice.gov.uk/. Registration is required, and code is freely available subject to completion of a software license.

https://doi.org/10.5194/bg-2022-229
Preprint. Discussion started: 20 December 2022

Author contributions

YG performed simulations and analysis, and wrote the first version of the manuscript. EJB prepared the model forcing data and set up the JULES suite. SEC and EJB are the developers of JULES and gave guidance on running JULES. MR assisted in using HIMMELI model. MA, LBF, KF, EH, AL, MBN and WP are the site PIs providing the site measurement data. ON provided the Sentinel-2 LAI data. AT and TL contributed to the statistical analysis of the work. HY helped on working with the supercomputer JASMIN. Funding acquisition was by YG and TA. TM, TA, EJB, and SEC contributed to the text of the manuscript.

Competing interests

The contact author has declared that neither they nor their co-authors have any competing interests.

Disclaimer

Publisher's note: Copernicus Publications remains neutral with regard to jurisdictional claims in published maps and institutional affiliations.

Acknowledgments

Olli Petola is ackowledged for preparing the daily methane flux data from the original site measured data. Jouni Susiluoto is acknowledged for giving instructions on using HIMMELI.

Financial Support

This work is mainly supported with the funding from the European Union's Horizon 2020 research and innovation programme under grant agreement 641816 (CRESCENDO) and the Maj ja Tor Nessling Foundation through the project "Resilience of high-latitude wetlands in a changing climate: modelling and evaluation of wetlands carbon sequestration and methane emissions" (Project number: 202000476). We would also like to thank The Strategic Research Council at the Academy of Finland (STN-SOMPA, 336573, STN-MULTA, 327214), MMM Grant No. 4400T-2105 (TURNEE), SA Grant No. 341752 (RESPEAT), 350184 (WINMET), EU-HORIZON ALFAWETLANDS (No. 101056844), EU-HORIZON ESM2025 (No. 101003536), and Business Finland Grant no. 6905/31/2018 for financial support. Funding for research in Kopytkowo, Poland was provided by the National Science Centre, Poland under project UMO-2020/37/B/ST10/01219 and University of Lodz under project 4/IDUB/DOS/2021.

References

Aurela, M., Lohila, A., Tuovinen, J.P., Hatakka, J., Penttilä, T. and Laurila, T.: Carbon dioxide and energy flux measurements in four northern-boreal ecosystems at Pallas, Boreal environmental research, 20, 455-473, 2015.

Aurela, M., Lohila, A., Tuovinen, J. P., Hatakka, J., Riutta, T., and Laurila, T.: Carbon dioxide exchange on a northern boreal fen, Boreal Environ. Res., 14, 699–710, https://doi.org/10.1093/treephys/tpn047, 2009.

https://doi.org/10.5194/bg-2022-229
Preprint. Discussion started: 20 December 2022

Aurela, M., Riutta, T., Laurila, T., Tuovinen, J.-P., Vesala, T., Tuittila, E.-S., Rinne, J., Haapanala, S., and Laine, J.: CO2 exchange of a sedge fen in southern Finland–the impact of a drought period, Tellus B, 59, 826–837, 2007.

Best, M.J., Pryor, M., Clark, D.B., Rooney, G.G., Essery, R., Ménard, C.B., Edwards, J.M., Hendry, M.A., Porson, A., Gedney, N. and Mercado, L.M.: The Joint UK Land Environment Simulator (JULES), model description–Part 1: energy and water fluxes, Geoscientific Model Development, 4(3), 677-699, 2011.

Brown, M. G., Humphreys, E. R., Moore, T. R., Roulet, N. T., and Lafleur, P. M.: Evidence for a nonmonotonic relationship between ecosystem- scale peatland methane emissions and water table depth. Journal of Geophysical Research: Biogeosciences, 119(5), 826-835, 2014.

Burke, E. J., Chadburn, S. E., and Ekici, A.: A vertical representation of soil carbon in the JULES land surface scheme (vn4.3_permafrost) with a focus on permafrost regions, Geoscientific Model Development, 10, 959– 975, doi:10.5194/gmd-10-959-2017,http://www.geosci-model-dev.net/10/959/2017/, 2017a.

Burke, E. J., Ekici, A., Huang, Y., Chadburn, S. E., Huntingford, C., Ciais, P., Friedlingstein, P., Peng, S., and Krinner, G.: Quantifying uncertainties of permafrost carbon–climate feedbacks, Biogeosciences, 14, 3051–3066, 2017b.

Ciais, P., Sabine, C., Bala, G., Bopp, L., Brovkin, V., Canadell, J., Chhabra, A., DeFries, R., Galloway, J., M., H., Jones, C., Le Quéré, C., Myneni, R. B., Piao, S., and Thornton, P.: Carbon and Other Biogeochemical Cycles, in: In Climate Change 2013: The Physical Science Basis. Contribution of Working Group I to the Fifth Assessment Report of IPCC, edited by: Stocker, T. F., Qin, D., Plattner, G.-K., Tignor, M., Allen, S. K., Boschung, J., Nauels, A., Xia, Y., Bex, V., and Midgley, P. M., Cambridge University Press, Cambridge, 2013.

Comyn-Platt, E., Hayman, G., Huntingford, C., Chadburn, S. E., Burke, E. J., Harper, A. B., Collins, W. J., Webber, C. P., Powell, T., Cox, P. M., Gedney, N., and Sitch, S.: Carbon budgets for 1.5 and 2 C targets lowered by natural wetland and permafrost feedbacks, Nature Geoscience, 11, 568, 2018.

Clark, D. B., Mercado, L. M., Sitch, S., Jones, C. D., Gedney, N., Best, M. J., Pryor, M., Rooney, G. G., Essery, R. L. H., Blyth, E., Boucher, O., Harding, R. J., Huntingford, C. and Cox, P. M.: The Joint UK Land Environment Simulator (JULES), model description–Part 2: carbon fluxes and vegetation dynamics, Geoscientific Model Development, 4(3), 701-722, doi:10.5194/gmd-4-701-2011, 2011.

Chadburn, S. E., Burke, E. J., Gallego-Sala, A. V., Smith, N. D., Bret-Harte, M. S., Charman, D. J., Drewer, J., Edgar, C. W., Euskirchen, E. S., Fortuniak, K., Gao, Y., Nakhavali, M., Pawlak, W., Schuur, E. A. G., and Westermann, S.: A new approach to simulate peat accumulation, degradation and stability in a global land surface scheme (JULES vn5.8_accumulate_soil) for northern and temperate peatlands, Geosci. Model Dev., 15, 1633–1657, https://doi.org/10.5194/gmd-15-1633-2022, 2022.

Chadburn, S.E., Aalto, T., Aurela, M., Baldocchi, D., Biasi, C., Boike, J., Burke, E.J., Comyn-Platt, E., Dolman, A.J., Duran- Rojas, C., Fan, Y., Friborg, T., Gao, Y., Gedney, N., Göckede, M., Hayman G.D., Holl D., Hugelius G., Kutzbach L., Lee H., Lohila A., Parmentier F.-J., Sachs T., Shurpali N.J., and Westermann S.: Modeled microbial dynamics explain the apparent temperature sensitivity of wetland methane emissions, Global Biogeochemical Cycles, 34(11), 2020.

Chadburn, S., Krinner, G., Porada, P., Bartsch, A., Beer, C., Belelli Marchesini, L., Boike, J., Ekici, A., Elberling, B., Friborg, T., Hugelius, G., Johansson, M., Kuhry, P., Kutzbach, L., Langer, M., Lund, M., Parmentier, F.-J. W., Peng, S., Van Huissteden, K., Wang, T., Westermann, S., Zhu, D., and Burke, E. J.: Carbon stocks and fluxes in the high latitudes: using site-level data to evaluate Earth system models, Biogeosciences, 14, 5143–5169, https://doi.org/10.5194/bg-14-5143-2017, https://www.biogeosciences.net/14/5143/2017/, 2017.

https://doi.org/10.5194/bg-2022-229
Preprint. Discussion started: 20 December 2022

Chadburn, S.E., Burke, E., Essery, R., Boike, J., Langer, M., Heikenfeld, M.,Cox, P., and Friedlingstein, P.: An improved representation of physical permafrost dynamics in the JULES land-surface model, Geosci. Model Dev., 8, 1493-1508, dohuangi:10.5194/gmd-8-1493-2015, 2015a.

Chadburn, S. E., Burke, E. J., Essery, R. L. H., Boike, J., Langer, M., Heikenfeld, M., Cox, P. M., and Friedlingstein, P.: Impact of model developments on present and future simulations of permafrost in a global land-surface model, The Cryosphere, 9, 1505-1521, doi:10.5194/tc-9-1505-2015, 2015b.

Chen, H., Xu, X., Fang, C., Li, B. and Nie, M.: Differences in the temperature dependence of wetland CO2 and CH4 emissions vary with water table depth. Nature Climate Change, 11(9), 766-771, 2021.

Denman, K. L., G. Brasseur, A. Chidthaisong, P. Ciais, P.M. Cox, R.E. Dickinson, D. Hauglustaine, C., Heinze, E. Holland, D. Jacob, U. Lohmann, S Ramachandran, P.L. da Silva Dias, Wofsy, S. C., and X. Zhang: Couplings Between Changes in the Climate System and Biogeochemistry, Cambridge University Press, Cambridge, United Kingdom and New York, NY, USA., 2007.

Dlugokencky, E. J., Bruhwiler, L., White, J. W. C., Emmons, L. K., Novelli, P. C., Montzka, S. A., Masarie, K. A., Lang, P. M., Crotwell, A. M., Miller, J. B., and Gatti, L. V.: Observational constraints on recent increases in the atmospheric CH4 burden, Geophysical Research Letters, 36(18), 2009.

Dorodnikov, M., Knorr, K. H., Kuzyakov, Y., and Wilmking, M.: Plant-mediated CH4 transport and contribution of photosynthates to methanogenesis at a boreal mire: a 14C pulse-labeling study, Biogeosciences, 8(8), 2365-2375, 2011.

Drebs, A., Nordlund, A., Karlsson, P., Helminen, J. and Rissanen, P.: Climatological statistics of Finland 1971-2000, Finnish Meteorological Institute, Helsinki, 99 ISBN 951-697-568-2, 2002.

Flanagan, L. B. and Syed, K. H.: Stimulation of both photosynthesis and respiration in response to warmer and drier conditions in a boreal peatland ecosystem, Glob. Change Biol., 17, 2271–2287, https://doi.org/10.1111/j.1365-2486.2010.02378.x, 2011.

Fortuniak, K., Pawlak, W., Siedlecki, M., Chambers, S., and Bednorz, L.: Temperate mire fluctuations from carbon sink to carbon source following changes in water table, Science of The Total Environment, 756, 144071, 2021.

Fortuniak, K., Pawlak, W., Bednorz, L., Grygoruk, M., Siedlecki, M., and Zieliński, M.: Methane and carbon dioxide fluxes of a temperate mire in Central Europe, Agr. Forest Meteorol., 232, 306–318, https://doi.org/10.1016/j.agrformet.2016.08.023, 2017.

Friedlingstein, P., Jones, M., O'Sullivan, M., Andrew, R., Hauck, J., Peters, G., Peters, W., Pongratz, J., Sitch, S., Le Quéré, C., others, and Zaehle, S.: Global carbon budget 2019, Earth System Science Data, 11, 1783–1838, 2019.

Global Soil Data Task Group: Global Gridded Surfaces of Selected Soil Characteristics (IGBP-DIS). [Global Gridded Surfaces of Selected Soil Characteristics (International Geosphere-Biosphere Programme - Data and Information System)]. Data set. Available on-line [http://www.daac.ornl.gov] from Oak Ridge National Laboratory Distributed Active Archive Center, Oak Ridge, Tennessee, U.S.A. doi:10.3334/ORNLDAAC/569, 2000.

Gedney, N., Huntingford, C., Comyn-Platt, E., and Wiltshire, A.: Significant feedbacks of wetland methane release on climate change and the causes of their uncertainty, Environmental Research Letters, 14, 084 027, 2019.

Gedney N, Cox P M, Huntingford C.: Climate feedback from wetland methane emissions. Geophysical Research Letters, 31(20), 2004.

Gedney N, Cox P M.: The sensitivity of global climate model simulations to the representation of soil moisture heterogeneity, Journal of Hydrometeorology, 4(6), 1265-1275, 2003.

Harper, A. B., Cox, P. M., Friedlingstein, P., Wiltshire, A. J., Jones, C. D., Sitch, S., Mercado, L. M., Groenendijk, M., Robertson, E., Kattge, J., Bönisch, G., Atkin, O. K., Bahn, M., Cornelissen, J., Niinemets, U., Onipchenko, V., Peñuelas, J., Poorter, L., Reich, P. B., Soudzilovskaia, N. A., and Bodegom, P. V.: Improved representation of plant functional types and

https://doi.org/10.5194/bg-2022-229
Preprint. Discussion started: 20 December 2022

physiology in the Joint UK Land Environment Simulator (JULES v4.2) using plant trait information, Geoscientific Model Development, 9, 2415–2440, https://doi.org/10.5194/gmd-9-2415-2016, https://www.geosci-model-dev.net/9/2415/2016/, 2016.

Huang, Y. Y., Ciais, P., Luo, Y., Zhu, D., Wang, Y., Qiu, C., Goll, D. S., Guenet, B., Makowski, D., De Graaf, I., Leifeld, J., Kwon, M. J., Hu, J., and Qu, L.: Tradeoff of CO2 and CH4 emissions from global peatlands under water-table drawdown, Nature climate change, 2021.

Knox, S. H., Jackson, R. B., Poulter, B., McNicol, G., Fluet-Chouinard, E., Zhang, Z., . . . Zona, D.: Fluxnet-CH4 synthesis activity: Objectives, observations, and future directions. Bulletin of the American Meteorological Society, 100 , 2607–2632. Retrieved from https://doi.org/10.1175/BAMS-D-18-0268.1, 2019.

Knox, S., Jackson, R. B., Poulter, B., McNicol, G., Fluet-Chouinard, E., Zhnag, Z., Hugelius, G., Bousuqet, P., canadell, J. G., Saunois , M., Papale, D., Chu, H., Keenan, T., Baldocchi, D., Tom, M. S., Trotta, C., Mammarella, I., Aurela, M., Bohrer, G., Campbell, D., Cescatti, A., Chamberlain, S., Chen, J., Chen, W., Dengel, S., Desai, A. R., Euskirchen, E., Friborg, T., Gasbarra, D., Goded, I., Goeckede, M., Heimann, M., Helbig, M., Hirano, T., Hollinger, D. Y., Iwata, H., Kang, M., Klatt, J., Kraus, K. W., Kutzbach, L. Lohila, A., Mitra, B., Morin, T. H., Nilsson, M. B., Niu, S., Noomets, A., Oechel, W. C., Peichl, M., Peltola, O., Reba, M. L., Runkle, B. R. K., Richardson, A. D., Ryu, Y., Sachs, T., Shcäfer, K. V. R., Scmid, H. P., Shurpali, N., Sonnentag, O., Tang, A. C. I., Ueyama, M., Vargas, R., Vesala, T., Ward, E. J., Windham-Myers, L., Wohlfahrt, G., and Zona, D.: FLUXNET-CH4 Synthesis Activity: Objectives, Observations, and Future Directions, Bulletin of the American Meteorological Society, 100(12), 2607-2632, 2019.

Lafleur, P. M., Moore, T. R., Roulet, N. T., and Frolking, S.: Ecosystem respiration in a cool temperate bog depends on peat temperature but not water table, Ecosystems, 8, 619–629, https://doi.org/10.1007/s10021-003-0131-2, 2005.

Lafleur, P. M., Roulet, N. T., J. L. Bubier, S. Frolking, and T. R. Moore: Interannual variability in the peatland-atmosphere carbon dioxide exchange at an ombrotrophic bog, Global Biogeochem. Cycles, 17(2), 1036, doi:10.1029/2002GB001983, 2003.

Larsson, A.: Holocene Carbon and nitrogen accumulation rates and contemporary carbon export in discharge, Licentiate Thesis, Swedish University of Agricultural Sciences. ISBN (print version) 978-91-576-9372-3, 2016.

Lohila, A., Aurela, M., Hatakka, J., Pihlatie, M., Minkkinen, K., Penttilä, T., and Laurila, T.: Responses of N2O fluxes to temperature, water table and N deposition in a northern boreal fen, European journal of soil science, 61(5), 651-661, 2010.

Long, K. D., Flanagan, L. B., and Cai, T.: Diurnal and seasonal variation in methane emissions in a northern Canadian peatland measured by eddy covariance, Glob. Change Biol., 16, 2420–2435, https://doi.org/10.1111/j.1365-2486.2009.02083.x, 2010.

Lupascu, M., Wadham, J. L., Hornibrook, E. R., and Pancost, R. D.: Temperature sensitivity of methane production in the permafrost active layer at Stordalen, Sweden: A comparison with non-permafrost northern wetlands. Arctic, Antarctic, and Alpine Research, 44(4), 469-482, 2012.

Mauder, M., Cuntz, M., Druee, C., Graf, A., Rebmann, C., Schmid, H. P., Schmidt, M., and Steinbrecher, R.: A strategy for quality and uncertainty assessment of long-term eddy-covariance measurements, Agr. Forest. Meteorol., 169, 122–135, https://doi.org/10.1016/j.agrformet.2012.09.006, 2013.

Mathijssen, P. J., Väliranta, M., Korrensalo, A., Alekseychik, P., Vesala, T., Rinne, J., and Tuittila, E. S. : Reconstruction of Holocene carbon dynamics in a large boreal peatland complex, southern Finland, Quaternary Science Reviews, 142, 1-15, 2016.

Mathijssen, P. J., Tuovinen, J. P., Lohila, A., Aurela, M., Juutinen, S., Laurila, T., Niemelä, E., Tuittila, E.-S. and Väliranta, M.: Development, carbon accumulation, and radiative forcing of a subarctic fen over the Holocene, The Holocene, 24(9), 1156-1166, 2014.

https://doi.org/10.5194/bg-2022-229
Preprint. Discussion started: 20 December 2022

Mauder, M., Cuntz, M., Druee, C., Graf, A., Rebmann, C., Schmid, H. P., Schmidt, M., and Steinbrecher, R.: A strategy for quality and uncertainty assessment of long-term eddy-covariance measurements, Agr. Forest. Meteorol., 169, 122–135, https://doi.org/10.1016/j.agrformet.2012.09.006, 2013.

Melton, J. R., Wania, R., Hodson, E. L., Poulter, B., Ringeval, B., Spahni, R., Bohn, T., Avis, C. A., Beerling, D. J., Chen, G., Elissev, A. V., Denisov, S. N., Hopcroft, P. O., Lettenmaier, D. P., Riley, W. J., Singarayer, J. S., Subin, Z. M., Tian, H., Zürcher, S., Brovkin, V., van Bodegom, P. M., Kleinen, T., Yu, Z. C., and Kaplan, J. O.: Present state of global wetland extent and wetland methane modelling: conclusions from a model inter-comparison project (WETCHIMP). Biogeosciences, 10(2), 753-788, 2013.

Moore, T. R., De Young, A., Bubier, J. L., Humphreys, E. R., Lafleur, P. M., and Roulet, N. T.: A multi-year record of methane flux at the Mer Bleue bog, southern Canada. Ecosystems, 14(4), 646-657, 2011.

Moore, T. R., Bubier, J. L., Frolking, S. E., Lafleur, P. M., and Roulet, N. T.: Plant biomass and production and CO_2 exchange in an ombrotrophic bog, J. Ecol., 90, 25–36, 2002.

Myhre, G., Shindell D., Bréon F.-M., Collins W., Fuglestvedt J., Huang J., Koch D., Lamarque J.-F., Lee D., Mendoza B., Nakajima T., Robock A., Stephens G., Takemura T., and Zhang H.: Anthropogenic and natural radiative forcing. In Climate Change 2013: The Physical Science Basis. Contribution of Working Group I to the Fifth Assessment Report of the Intergovernmental Panel on Climate Change. T.F. Stocker, D. Qin, G.-K. Plattner, M. Tignor, S.K. Allen, J. Doschung, A. Nauels, Y. Xia, V. Bex, and P.M. Midgley, Eds. Cambridge University Press, pp. 659-740, doi:10.1017/CBO9781107415324.018, 2013.

Nevalainen, O.: ollinevalainen/satellitetools: v1.0.0 (v1.0.0), Zenodo, https://doi.org/10.5281/zenodo.5993292, 2022.

Nilsson, M. and Öquist, M.: Partitioning litter mass loss into carbon dioxide and methane in peatland ecosystems, Geoph. Monog. Series, Carbon Cycling in Northern Peatlands, 184, 131–144, 2009.

Nilsson, M., Sagerfors, J., Buffam, I., Laudon, H., Eriksson, T., Grelle, A., Klemedtsson, L., Weslien, P., and Lindroth, A.: Contemporary carbon accumulation in a boreal oligotrophic minerogenic mire–a significant sink after accounting for all C- fluxes, Global Change Biology, 14(10), 2317-2332, 2008.

Osterwalder S., Bishop, K., Alewell, C., Fritsche, J., Laudon, H., Åkerblom, S., & Nilsson, M. B.: Mercury evasion from a boreal peatland shortens the timeline for recovery from legacy pollution, Scientific Reports, 7(1), 1-9, 16022, https://doi.org/10.1038/s41598-017-16141-7, 2017.

Peltola, O., Vesala, T., Gao, Y., Räty, O., Alekseychik, P., Aurela, M., Chojnicki, B., Desai, A. R., Dolman, A. J., Euskirchen, E. S., Friborg, T., Göckede, M., Helbig, M., Humphreys, E., Jackson, R. B., Jocher, G., Joos., F., Klatt, J., Knox, S. H., Kowalska, N., Kutzbach, L., Lienert, S., Lohila, A., Mammarella, I., Nadeau, D. F., Nilsson, M. B., Oechel, W. C., Peichl M., Pypker T., Quinton W., Rinne, J., Sachs, T., Samson, M., Schmid, H. P., Sonnentag, O., Wille, C., Zona, D., and Aalto, T.: Monthly gridded data product of northern wetland methane emissions based on upscaling eddy covariance observations. Earth System Science Data, 11(3), 1263-1289, 2019.

Pirinen, P., Simola, H., Aalto, J., Kaukoranta, J. P., Karlsson, P., & Ruuhela, R.: Tilastoja Suomen ilmastosta 1981-2010, [Climatological statistics of Finland 1981-2010.], Finnish Meteorological Institute, reports 1/2012, Helsinki, 83 pp. Finnish with English summary, 2012.

Raivonen, M., Smolander, S., Backman, L., Susiluoto, J., Aalto, T., Markkanen, T., Mäkelä J, Rinne J, Peltola O, Aurela M, Tomasic, M., Li X.F., Larmola, T., Juutinen, S., Tuittila, E.-S., Heimann, M., Sevanto, S., Kleinen, T., Brovkin V. and Vesala, T.: HIMMELI v1. 0: HelsinkI Model of MEthane buiLd-up and emIssion for peatlands, Geoscientific Model Development, 10, 4665-4691, 2017.

https://doi.org/10.5194/bg-2022-229
Preprint. Discussion started: 20 December 2022

Rosenzweig, C., Arnell, N. W., Ebi, K. L., Lotze-Campen, H., Raes, F., Rapley, C., Smith, M. S., Cramer, W., Frieler, K., Reyer, C. P., Schewe, J., van Vuuren, D., and Warszawski, L.: Assessing inter-sectoral climate change risks: the role of ISIMIP, Environmental Research Letters, 12, 010 301, 2017.

Rinne, J., Tuittila, E.-S., Peltola, O., Li, X., Raivonen, M., Alekseychik, P., Haapanala, S., Pihlatie, M., Aurela, M., Mammarella, I., and Vesala, T.: Temporal Variation of Ecosystem Scale Methane Emission From a Boreal Fen in Relation to Temperature, Water Table Position, and Carbon Dioxide Fluxes, Global Biogeochem. Cy., 32, 1087–1106, https://doi.org/10.1029/2017GB005747, 2018.

Rinne, J., Riutta, T., Pihlatie, M., Aurela, M., Haapanala, S., Tuovinen, J.-P., Tuittila, E.-S., Vesala, T.: Annual cycle of methane emission from a boreal fen measured by the eddy covariance technique, Tellus Ser. B Chem. Phys. Meteorol. 59, 449–457. (doi:10. 1111/j.1600-0889.2007.00261.x), 2007.

Riley, W. J., Subin, Z. M., Lawrence, D. M., Swenson, S. C., Torn, M. S., Meng, L., Mahowald, N. M., and Hess, P.: Barriers to predicting changes in global terrestrial methane fluxes: analyses using CLM4Me, a methane biogeochemistry model integrated in CESM, Biogeosciences, 8, 1925–1953, https://doi.org/10.5194/bg-8-1925-2011, 2011.

Roulet, N. T., Lafleur, P. M., Richard, P. J., Moore, T. R., Humphreys, E. R., and Bubier, J.: Contemporary carbon balance and late holocene carbon accumulation in a northern peatland, Global Change Biol., 13, 397–411, 2007.

Sagerfors, J., Lindroth, A., Grelle, A., Klemedtsson, L., Weslien, P., and Nilsson, M. B.: Annual CO2 exchange between a nutrient-poor, minerotrophic, boreal mire and the atmosphere, J. Geophys. Res.-Biogeo., 113, 1–15, https://doi.org/10.1029/2006JG000306, 2008.

Saunois, M., Stavert, A. R., Poulter, B., Bousquet, P., Canadell, J. G., Jackson, R. B., Raymond, P. A., Dlugokencky, E. J., Houweling, S., Patra, P. K., Ciais, P., Arora, V. K., Bastviken, D., Bergamaschi, P., Blake, D. R., Brailsford, G., Bruhwiler, L., Carlson, K. M., Carrol, M., Castaldi, S., Chandra, N., Crevoisier, C., Crill, P. M., Covey, K., Curry, C. L., Etiope, G., Frankenberg, C., Gedney, N., Hegglin, M. I., Höglund-Isaksson, L., Hugelius, G., Ishizawa, M., Ito, A., Janssens-Maenhout, G., Jensen, K. M., Joos, F., Kleinen, T., Krummel, P. B., Langenfelds, R. L., Laruelle, G. G., Liu, L., Machida, T., Maksyutov, S., McDonald, K. C., McNorton, J., Miller, P. A., Melton, J. R., Morino, I., Müller, J., Murguia-Flores, F., Naik, V., Niwa, Y., Noce, S., O'Doherty, S., Parker, R. J., Peng, C., Peng, S., Peters, G. P., Prigent, C., Prinn, R., Ramonet, M., Regnier, P., Riley, W. J., Rosentreter, J. A., Segers, A., Simpson, I. J., Shi, H., Smith, S. J., Steele, L. P., Thornton, B. F., Tian, H., Tohjima, Y., Tubiello, F. N., Tsuruta, A., Viovy, N., Voulgarakis, A., Weber, T. S., van Weele, M., van der Werf, G. R., Weiss, R. F., Worthy, D., Wunch, D., Yin, Y., Yoshida, Y., Zhang, W., Zhang, Z., Zhao, Y., Zheng, B., Zhu, Q., Zhu, Q., and Zhuang, Q.: The Global Methane Budget 2000–2017, Earth System Science Data, 12, 1561–1623, https://doi.org/10.5194/essd-12-1561-2020, 2020.

Saunois, M., Bousquet, P., Poulter, B., Peregon, A., Ciais, P., Canadell, J. G., Dlugokencky, E. J., Etiope, G., Bastviken, D., Houweling, S., Janssens-Maenhout, G., Tubiello, F. N., Castaldi, S., Jackson, R. B., Alexe, M., Arora, V. K., Beerling, D. J., Bergamaschi, P., Blake, D. R., Brailsford, G., Brovkin, V., Bruhwiler, L., Crevoisier, C., Crill, P., Covey, K., Curry, C., Frankenberg, C., Gedney, N., Höglund-Isaksson, L., Ishizawa, M., Ito, A., Joos, F., Kim, H. S., Kleinen, T., Krummel, P., Lamarque, J. F., Langenfelds, R., Locatelli, R., Machida, T., Maksyutov, S., McDonald, K. C., Marshall, J., Melton, J., R., Morino, I., Naik, V., O'Doherty, S., Parmentier, F. J. W., Patra, P. K., Peng, C., Peng, S., Peters, G. P., Pison, I., Prigent, C., Prinn, R., Ramonet, M., Riley, W. J., Saito, M., Santini, M., Schroeder, R., Simpson, I. J., Spahni, R., Steele, P., Takizawa, A., Thornton, B. F., Tian, H., Tohjima, Y., Viovy, N., Voulgarakis, A., van Weele, M., van der Werf, G. R., Weiss, R., Wiedinmyer, C., Wilton, D. J., Wiltshire, A., Worthy, D., Wunch, D., Xu, X., Yoshida, Y., Zhang, B., Zhang, Z., and Zhu, Q.: The global methane budget 2000–2012, Earth Syst. Sci. Data, 8, 697-751, doi :10.5194/essd-8-697-2016, 2016.

https://doi.org/10.5194/bg-2022-229
Preprint. Discussion started: 20 December 2022

Segers, R.: Methane production and methane consumption: a review of processes underlying wetland methane fluxes, Biogeochemistry, 41, 23–51, 1998.

Sellar, A. A., Jones, C. G., Mulcahy, J., Tang, Y., Yool, A., Wiltshire, A., O'connor, F. M., Stringer, M., Hill, R., Palmieri, J., others, and Zerroukat, M.: UKESM1: Description and evaluation of the UK Earth System Model, Journal of Advances in Modeling Earth Systems, 11, 4513–4558, 2019.

Smith, N. D., Burke, E. J., Schanke Aas, K., Althuizen, I. H. J., Boike, J., Christiansen, C. T., Etzelmüller, B., Friborg, T., Lee, H., Rumbold, H., Turton, R. H., Westermann, S., and Chadburn, S. E.: Explicitly modelling microtopography in permafrost landscapes in a land surface model (JULES vn5.4_microtopography), Geoscientific Model Development, 15(9), 3603-3639, 2022.

Song, C., Luan, J., Xu, X., Ma, M., Aurela, M., Lohila, A., Mammarella, I., Alekseychik, P., Tuittila, E.-S., Gong, W., Chen, X., Meng, X., and Yuan, W.: A microbial functional group based CH4 model integrated into a terrestrial ecosystem model: Model structure, site level evaluation, and sensitivity analysis. Journal of Advances in Modeling Earth Systems, 12, e2019MS001867. https://doi.org/10.1029/2019MS001867, 2020.

Tang, J., Zhuang, Q., Shannon, R. D., and White, J. R.: Quantifying wetland methane emissions with process-based models of different complexities, Biogeosciences, 7, 3817–3837, https://doi.org/10.5194/bg-7-3817-2010, 2010.

Treat, C. C., Bloom, A. A., and Marushchak, M. E.: Nongrowing season methane emissions–a significant component of annual emissions across northern ecosystems, Global Change Biology, 24(8), 3331-3343, 2018.

Turetsky, M. R., Kotowska, ,,,,A., Bubier, J., Dise, N. B., Crill, P., Hornibrook, E. R., Minkkinen K., Moore T. R., Myers-Smith I. H., Nykänen H., Olefeldt D., Rinne J., Saarnio S., Shurpali N., Tuittila E-S., Waddington J. M., White J. R., Wickland K. P. and Wilmking, M: A synthesis of methane emissions from 71 northern, temperate, and subtropical wetlands, Global change biology, doi: 10.1111/gcb.12580, 2014.

Watson, A., Stephen, K. D., Nedwell, D. B., and Arah, J. R. M.:Oxidation of methane in peat: Kinetics of CH4 and O2 removal and the role of plant roots, Soil Biol. Biochem., 29, 1257–1267, 1997.

Weedon, G.P., Balsamo, G., Bellouin, N., Gomes, S., Best, M.J. and Viterbo, P.: The WFDEI meteorological forcing data set: WATCH Forcing Data methodology applied to ERA- Interim reanalysis data, Water Resources Research, 50(9), pp.7505-7514, 2014.

Weedon, G.P., Gomes, S., Viterbo, P., Österle, H., Adam, J.C., Bellouin, N., Boucher, O., and Best, M.: The WATCH forcing data 1958-2001: A meteorological forcing dataset for land surface- and hydrological- models, WATCH technical report, 2010.

Weiss, M. and Baret, F.: S2ToolBox Level 2 products: LAI, FAPAR, FCOVER, available at: https://step.esa.int/docs/extra/ATBD_S2ToolBox_L2B_V1.1.pdf, 2016.

Whalen, S. C. and Reeburgh, W. S.: Moisture and temperature sensitivity of CH4 oxidation in boreal soils, Soil Biol. Biochem., 28, 1271–1281, 1996.

Wiltshire, A. J., Burke, E. J., Chadburn, S. E., Jones, C. D., Cox, P. M., Davies-Barnard, T., Friedlingstein, P., Harper, A. B., Liddicoat, S., Sitch, S., and Zaehle, S.: JULES-CN: a coupled terrestrial carbon–nitrogen scheme (JULES vn5.1), Geoscientific Model Development, 14, 2161–2186, https://doi.org/10.5194/gmd-14-2161-2021, https://gmd.copernicus.org/articles/14/2161/2021/, 2021.

Xu, X., Yuan, F., Hanson, P. J., Wullschleger, S. D., Thornton, P. E., Riley, W. J., Song, X., Graham, D. E., Song, C., and Tian, H.: Reviews and syntheses: Four decades of modeling methane cycling in terrestrial ecosystems. Biogeosciences, 13(12), 3735-3755, 2016.

https://doi.org/10.5194/bg-2022-229
Preprint. Discussion started: 20 December 2022

Yvon-Durocher, G., Allen, A. P., Bastviken, D., Conrad, R., Gudasz, C., St-Pierre, A., Thanh-Duc N. and Del Giorgio, P. A.: Methane fluxes show consistent temperature dependence across microbial to ecosystem scales, Nature, 507 (7493), 488, 2014.

Zhang, H., Tuittila, E.-S., Korrensalo, A., Laine, A. M., Uljas, S., Welti, N., Kerttula, J., Maljanen, M., Elliott, D., Vesala, T., and Lohila, A.: Methane production and oxidation potentials along a fen- bog gradient from southern boreal to subarctic peatlands in Finland, Global Change Biology, 27(18), 4449-4464, 2021.

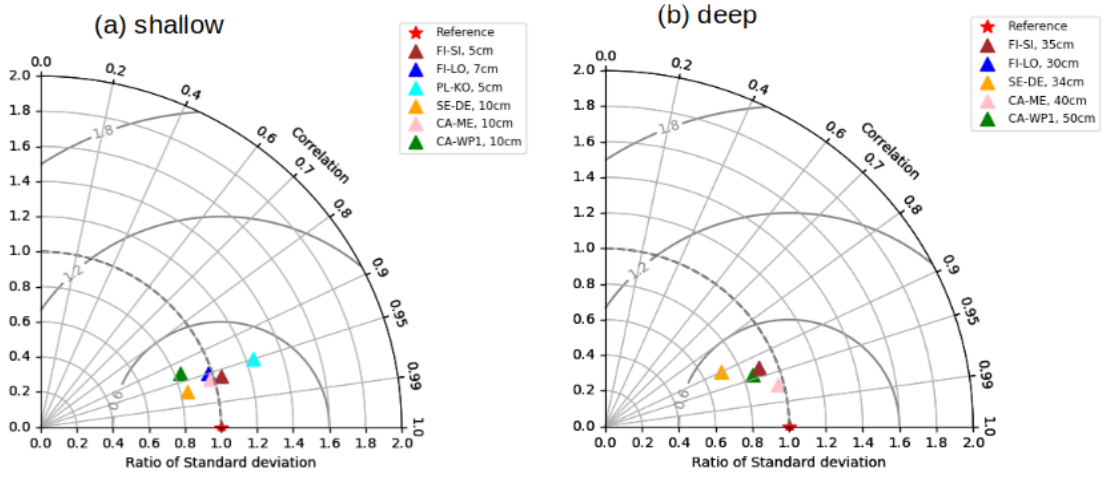

Figure 1: Taylor diagrams of soil temperatures at (a) shallow (5-10cm) and (b) deeper (34-50cm) soil depths. All statistics were calculated using daily averaged data. All points were normalized by dividing the standard deviation of model results by the standard deviation of the corresponding measurements; thus, the reference point is 1.0. Sites are represented with different colors. For the Kopytkowo site, the measured soil temperature is only collected at 5cm. (The time series of observed and simulated soil temperatures at sites are shown in Figure S1 in supplementary).

https://doi.org/10.5194/bg-2022-229
Preprint. Discussion started: 20 December 2022

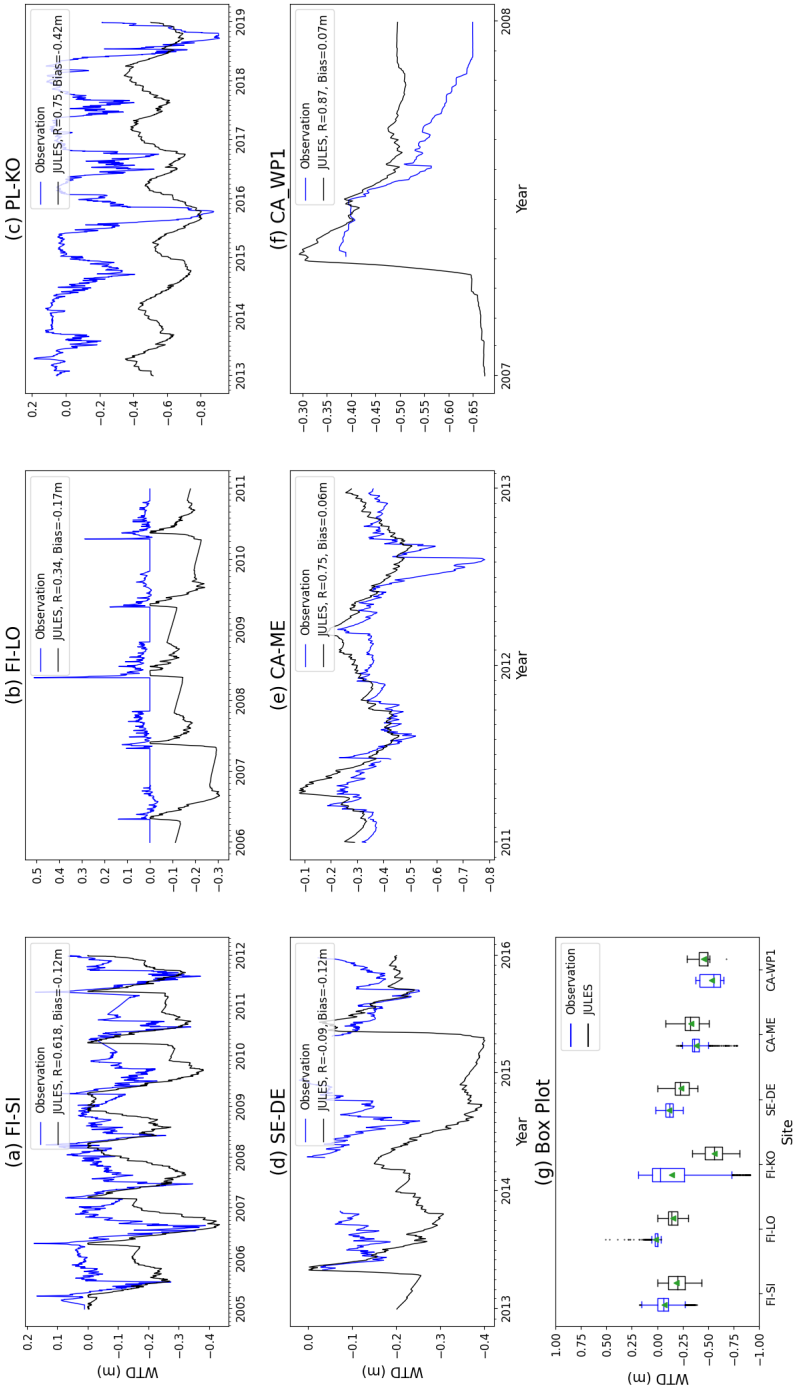

Figure 2: Simulated and observed daily water table depth (WTD) at each site. The box plot shows the median (line), mean value (green triangle), Q1 (25%) and Q3 (75%) quartiles of the data (the bottom and top of the box), and the lower and upper whiskers represent the range of 1.5 times interquartile range (Q3-Q1) from the Q1 and Q3. The data points outside the 1.5 times interquartile range can be considered as extremes. The same period as the observed methane flux was selected for the observed WTD data, and the statistics shown in the figure were calculated by filtering the simulated WTD according to the availability of observed WTD.

https://doi.org/10.5194/bg-2022-229
Preprint. Discussion started: 20 December 2022

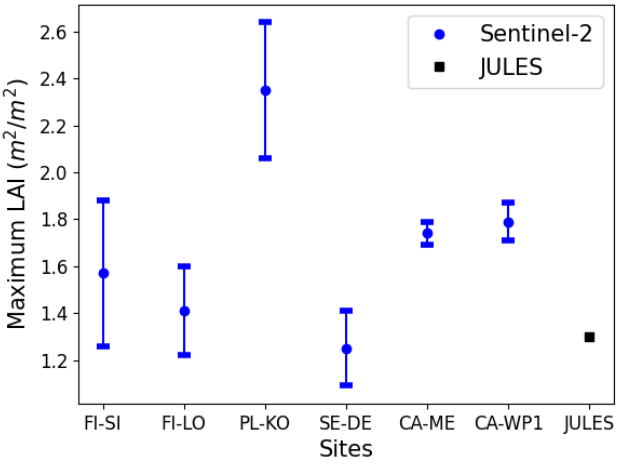

Figure 3: Maximum leaf area index (LAI) and its standard deviation over the selected area from Sentinel-2 satellite data for each site, and the maximum LAI used for the JULES simulations for all the sites.

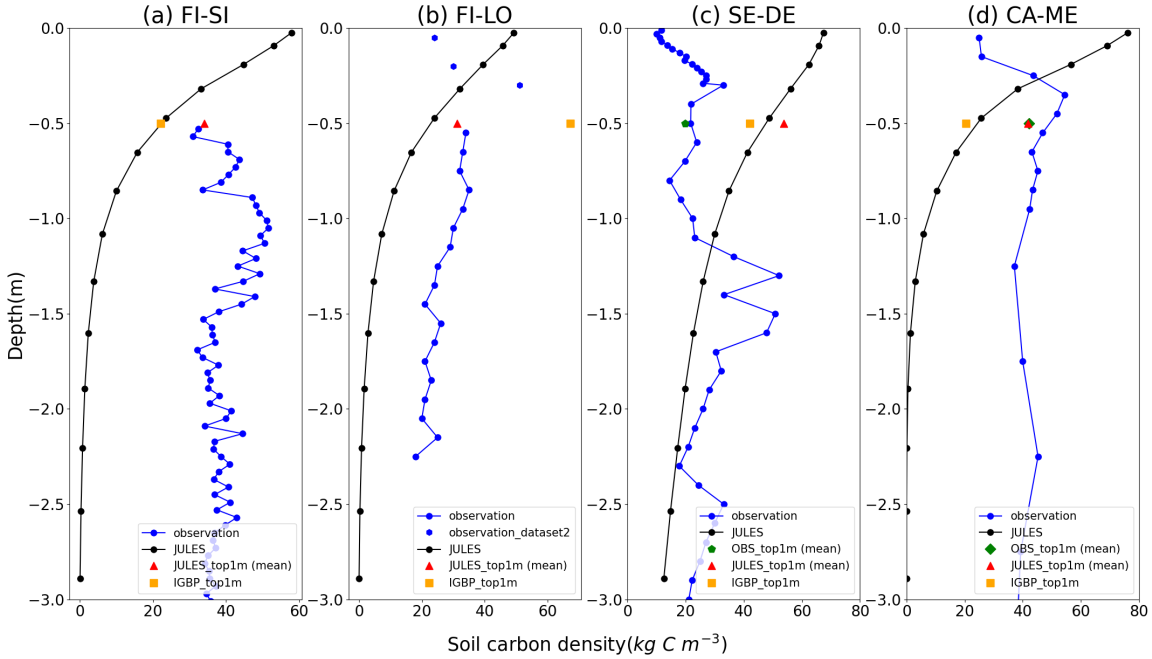

760

Figure 4: Comparison between simulated and observed soil carbon density profiles at Siikaneva Fen, Lompolojänkkä, Degerö, Mer Bleue sites. The OBS_top1m (mean) in (c) and (d) means the averaged soil carbon density of the top 1 meter soil from observation. The JULES_top1m (mean) and IGBP_top1m represent the averaged soil carbon density of the top 1 meter soil from JULES simulation and IGBP dataset, respectively.

https://doi.org/10.5194/bg-2022-229
Preprint. Discussion started: 20 December 2022

Biogeosciences
Discussions
Open Access
EGU

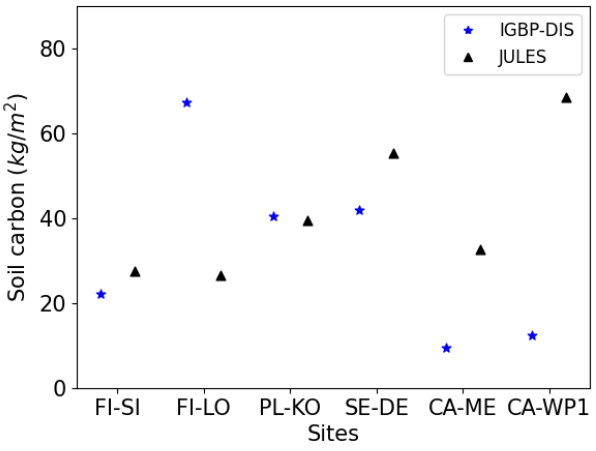

765

Figure 5: Comparison between JULES simulated soil carbon and IGBP soil carbon data at top 1 meter of soil.

https://doi.org/10.5194/bg-2022-229
Preprint. Discussion started: 20 December 2022

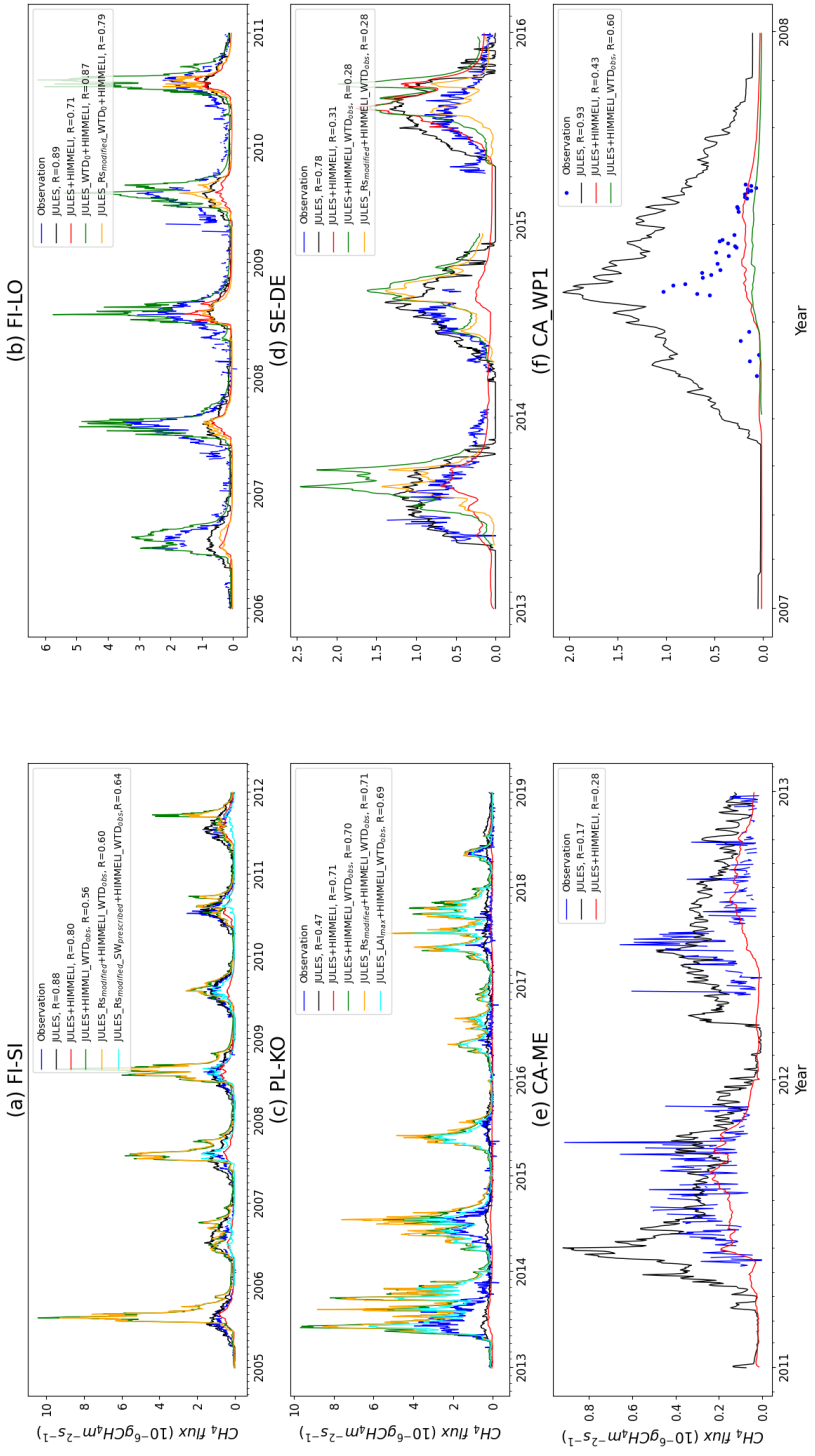

Figure 6: Comparison of simulated methane (CH_4) fluxes from different simulation setups (introduced in section 2.3.3) with site observed CH_4 fluxes at daily time scale.

https://doi.org/10.5194/bg-2022-229
Preprint. Discussion started: 20 December 2022

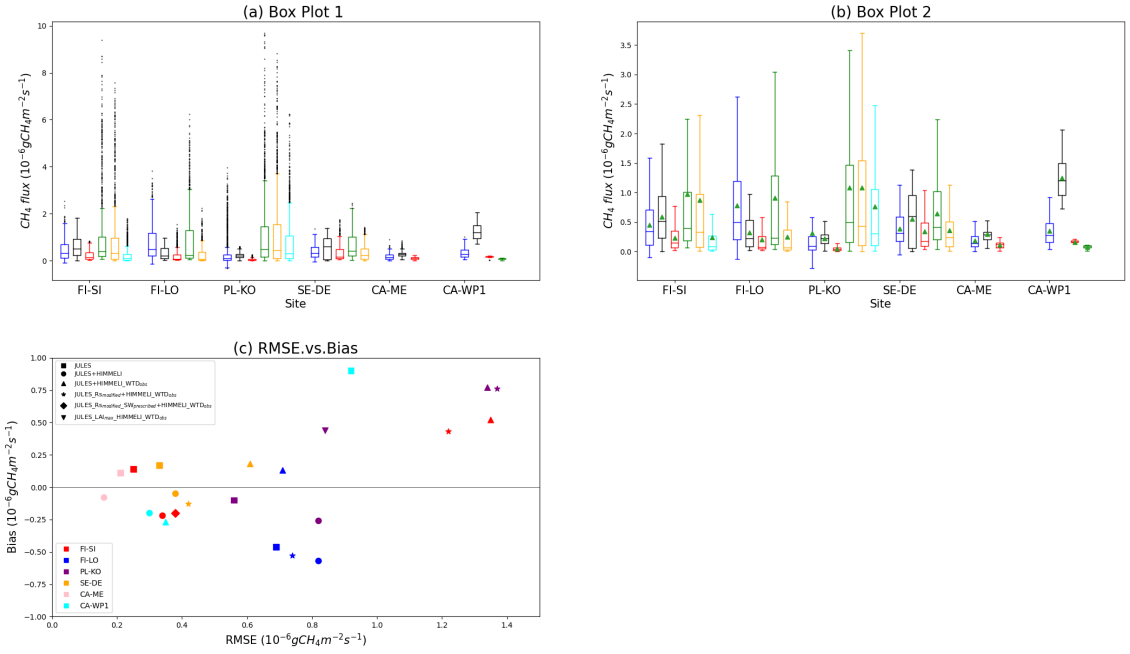

Figure 7: The box plots show the median (line), mean (green triangle), 25% (Q1) and 75% (Q3) quartiles (the top and bottom of the box) of the observed and simulated methane (CH_4) fluxes at the studied sites, and the whiskers represent the range of 1.5 times interquartile range (Q3-Q1) from the Q1 and Q3. The data points outside the whiskers are shown in (a) Box Plot 1, and the mean values are shown in (b) Box Plot 2. The colors of boxes follow the legends of observed and simulated CH_4 fluxes of each site in Fig. 6. The root mean square error (RMSE) and bias of the model simulations (represented by different shapes) for all the studied sites (represented by different colors) are shown in (c) RMSE vs. Bias figure. All the statistics were calculated according to the availability of observed CH_4 fluxes.

https://doi.org/10.5194/bg-2022-229
Preprint. Discussion started: 20 December 2022

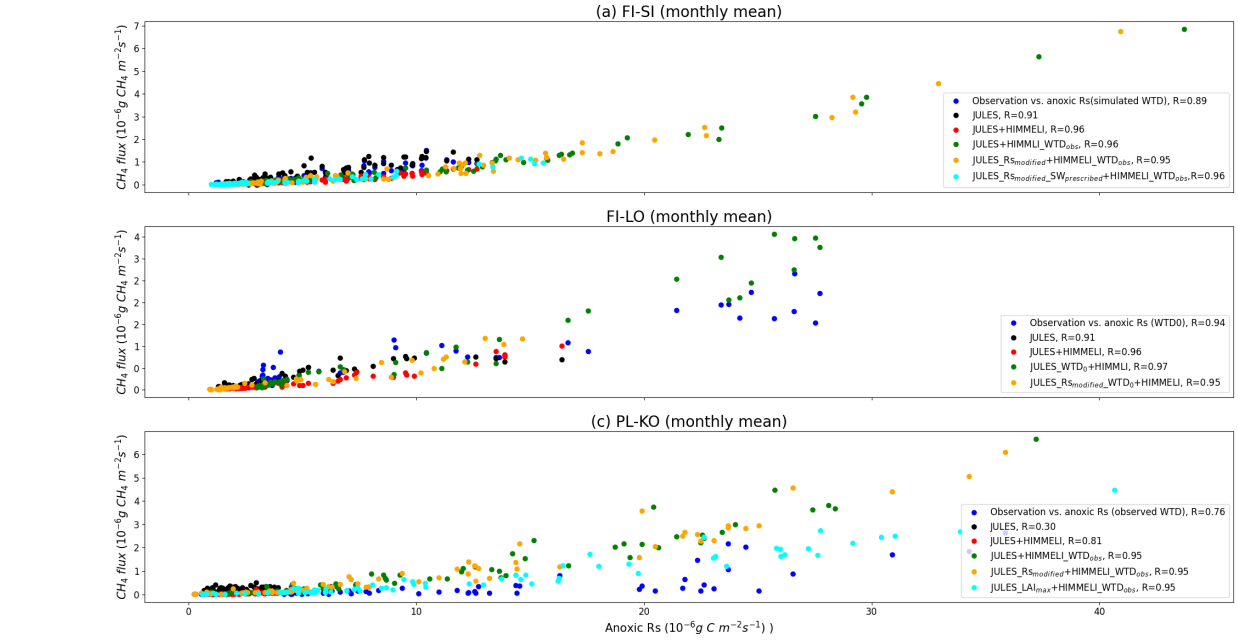

780 **Figure 8: Monthly means of methane (CH_4) fluxes against the rate of anoxic soil respiration (anoxic Rs) at Siikaneva, Kopytkowo and Lompolojänkkä. Simulated anoxic Rs is presented as there is no observed anoxic Rs available.**

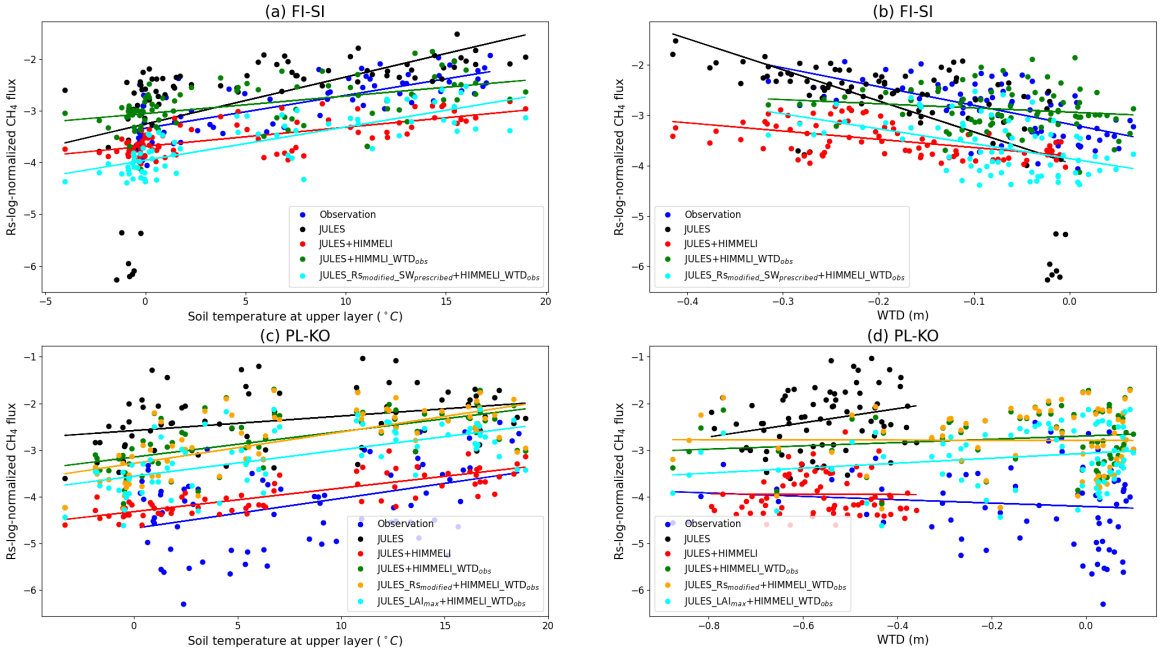

Figure 9: Comparison of the relationships between monthly means of upper layer soil temperature and Rs-log-normalized methane (CH_4) emissions (log normalization of the ratio of CH4 emission to anoxic Rs rate), also the relationships between monthly means of
785 **water table depth (WTD) and Rs-log-normalized CH_4 emissions from both observations and simulations at Siikaneva and Kopytkowo site.**

https://doi.org/10.5194/bg-2022-229
Preprint. Discussion started: 20 December 2022

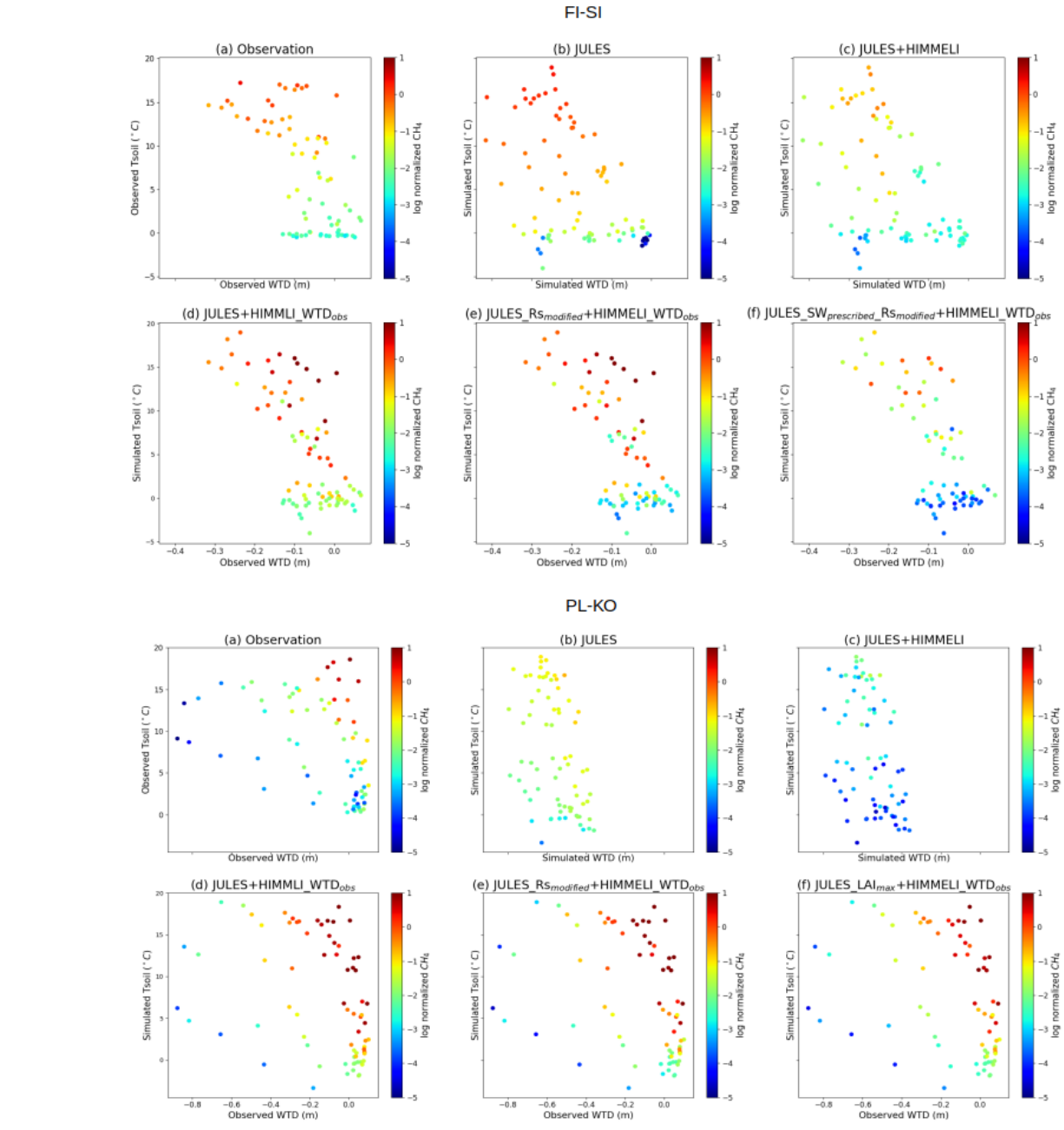

Figure 10: Responses of log-normalized methane (CH_4) fluxes to surface soil temperature (Tsoil) and water table depth (WTD) from observation and simulations for Siikaneva and Kopytkowo sites. Circles refer to monthly mean values during 2005–2011 and 2013-2019 for Siikaneva and Kopytkowo sites, respectively.

https://doi.org/10.5194/bg-2022-229
Preprint. Discussion started: 20 December 2022

Biogeosciences Discussions Open Access EGU

Table 1: Site characteristics of studied wetland sites.

Sites (Abbre.)	Lat., Long.	Climate Zone	Wetland type	Peat depth (m)	Dominant Vegetation	Climate (average temp. and precip.)	Data resolution and period	Reference
Siikaneva (FI-SI)	61.8 °N 24.2°E	Boreal	Oligotrophic (nutrient poor) Fen	2-4	Sedges, Rannoch-rush, peat mosses	3.3 °C and 713 mm	30 min, 2005-2012	Aurela et al. (2007), Rinne et al. (2018)
Lompolojänkkä (FI-LO)	68.0 °N 24.2 °E	Boreal	Minerotrophic (mesotrophic (nutrient rich) Fen	2-3	Moss cover 57%, sedges, birch, willow	-1.4 °C and 484 mm	30 min, 2006-2010	Aurela et al. (2015, 2009)
Degerö Stormyr (SE-DE)	64.2 °N 19.6 °E	Boreal	Minerogenic Oligotrophic (nutrient poor) Fen (a mixed acid mire)	3-4 m on average, up to 8m	Sedges and mosses	1.2 °C and 523 mm	30 min, 2013-2015	Sagerfors et al. (2008)
Kopytkowo (PL-KO)	53.6 °N 22.9 °E	Temperate	Fen (mire)	2.5	Mixture of reeds, sedges, and rushes	6.6 °C and 583 mm	Houly, 2013-2018	Fortuniak et al. (2017, 2021)
Mer Bleue (CA-ME)	45.4°N -75.5 °E	Temperate	Ombrotrophic bog	5-6 m at the center, 0.3m at the margins	Dominant low status evergreen and deciduous shrubs, sparse cover of sedges and a few small trees, underlying moss	6.4+/- 0.8 °C and 943 mm	Daily, 2011-2012	Lafleur et al. (2005), Moore et al. (2011), Brown et al. (2014)
Western Peatland 1 (CA-WP1)	55.0 °N - 112.5 °E	Temperate	Moderately 'rich' treed Fen	~2	Dominated by stunted trees, with high abundance of a shrub, and a wide range of moss species.	2.1 °C and 504 mm	30 min, 2007	Long et al. (2010), Flanagan and Syed (2011)

795

https://doi.org/10.5194/bg-2022-229
Preprint. Discussion started: 20 December 2022

Table 2: Model simulations performed in this study.

	Experiment	Model setup
Site common run	JULES	Results from the JULES default methane module (with the layered soil temperature scheme switched on and the microbial methane production scheme switched off)
	JULES+HIMMELI	HIMMELI simulation using JULES model results as HIMMELI inputs. JULES simulated soil temperature, LAI, the rate of total soil respiration, WTD were used. The rate of anoxic soil respiration (anoxic Rs) for HIMMELI was calculated as the rate of total soil respiration below the simulated WTD.
	JULES + HIMMELI_WTD_{obs}	HIMMELI simulation using JULES results as inputs. Observed water table depth (WTD_{obs}) was used instead of JULES simulated WTD. The rate of anoxic Rs for HIMMELI was calculated as the rate of total soil respiration below WTD_{obs}. Note that in this way, the JULES simulated soil temperature is inconsistent with WTD_{obs}, and the total soil respiration at soil layers above the JULES WTD could include contribution from oxic soil respiration. Nevertheless, we consider the rate of anoxic Rs as the total soil respiration rate below WTD_{obs} here because JULES does not simulate oxic and anoxic soil respiration separately.
	JULES_$Rs_{modified}$+ HIMMELI_WTD_{obs}	JULES run with the modified soil carbon decomposition rate. Other settings followed JULES + HIMMELI_WTD_{obs}.
Site specific run	JULES_$Rs_{modified}$_$SW_{prescribed}$ + HIMMELI_WTD_{obs}	WTD_{obs} was used to prescribe the soil moisture content in JULES. For the JULES soil layers above observed WTD, soil moisture content is equal to the JULES simulated soil moisture content. For the JULES soil layers below WTD, soil moisture content equals 1 i.e., saturated soil. The modified soil carbon decomposition rate was used in JULES. WTD_{obs} was used in HIMMELI. The simulation was done for the **Siikaneva** site only.
	JULES_WTD_0+ HIMMELI	The entire soil column was set to be saturated, thus the WTD in JULES equals zero. This was done for the **Lompolojänkkä** site only.
	JULES_LAI_{max} + HIMMELI_WTD_{obs}	The maximum LAI in JULES was set to be 2.35 instead of 1.3. WTD_{obs} was used in HIMMIELI. This simulation was done for the **Kopytkowo** site only.

https://doi.org/10.5194/bg-2022-229
Preprint. Discussion started: 20 December 2022

Table 3: Standard deviation of annual means of methane emissions (10^{-6}g CH_4 $m^{-2}s^{-1}$) from observation and simulations for Siikaneva, Lompolojänkkä and Kopytkowo sites. Results are only shown for those three sites with better data coverage throughout the study periods.

Site	Standard Deviation					
Siikaneva	Obs.	JULES	JULES+ HIMMELI	JULES + HIMMELI_WTD$_{obs}$	JULES_Rs$_{modified}$+ HIMMELI_WTD$_{obs}$	JULES_Rs$_{modified}$_SW$_{prescribed}$ + HIMMELI_WTD$_{obs}$
	0.0998	0.0370	0.0447	0.3020	0.2826	0.0833
Lompolojänkkä	Obs.	JULES	JULES+ HIMMELI	JULES_WTD$_0$ + HIMMELI	JULES_Rs$_{modified}$_WTD$_0$+ HIMMELI	
	0.0826	0.0176	0.0564	0.0630	0.0684	
Kopytkowo	Obs.	JULES	JULES+ HIMMELI	JULES + HIMMELI_WTD$_{obs}$	JULES_Rs$_{modified}$+ HIMMELI_WTD$_{obs}$	JULES_LAI$_{max}$ + HIMMELI_WTD$_{obs}$
	0.3144	0.0381	0.0254	0.7226	0.7018	0.4794